On the strength of transversely isotropic rocks

Ronaldo I. Borja
Stanford University

28 - 29 March, 2019 Madrid, Spain

STAMS 2019

First Colloquium of the Spanish Theoretical and Applied Mechanics Society

March 29, 2019

A serendipitous meeting with Enrique

Una fructífera colaboración

Borja, R. I. and Alarcón, E., “A mathematical framework for finite strain elastoplastic consolidation, Part 1: Balance laws, variational formulation, and linearization,” Computer Methods in Applied Mechanics and Engineering, Vol. 122, Nos. 1-2, 1995, pp. 145-171.

Borja, R.I., Tamagnini, C. and Alarcón, E., “Finite strain elastoplastic consolidation, Part 2: Finite element implementation and numerical examples,” Computer Methods in Applied Mechanics and Engineering, Vol. 159, Nos. 1-2, 1998, pp. 103-122.

Borja, R. I. and Alarcón, E., “Un marco matemático para la consolidación elastoplástica con deformaciones finitas,” Revista Internacional de Métodos Numéricos para Cálculo y Diseño en Ingeniería, Vol. 11, No. 3, 1995, pp. 345-381

Borja, R. I., Tamagnini, C. and Alarcón, E., “Consolidación elastoplástica con deformaciones finitas: implementación con elementos finitos y ejemplos numéricos,” Revista Internacional de Métodos Numéricos para Cálculo y Diseño en Ingeniería, Vol. 15, No. 2, 1999, pp. 269-296.

Outline of presentation

Part 1:
Dual porosity/dual permeability theory (Borja and Choo, CMAME, 2016)

Part 2:
Transversely isotropic rocks, (Semnani et al., IJNAMG 2016, Zhao et al., IJNAMG 2018)

Integration of Parts 1 and 2: US Department of Energy project, in progress.

Double porosity

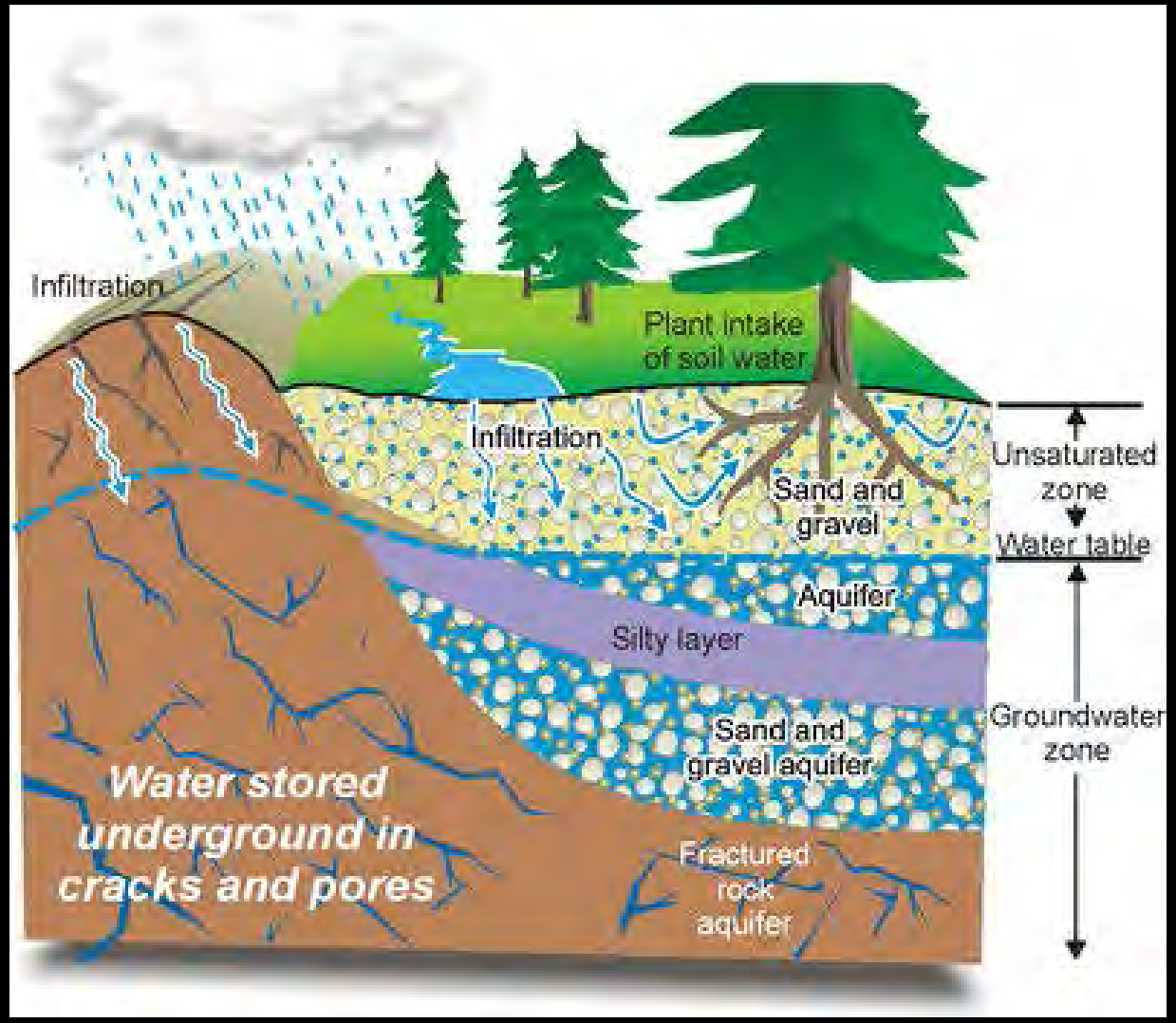

Double porosity

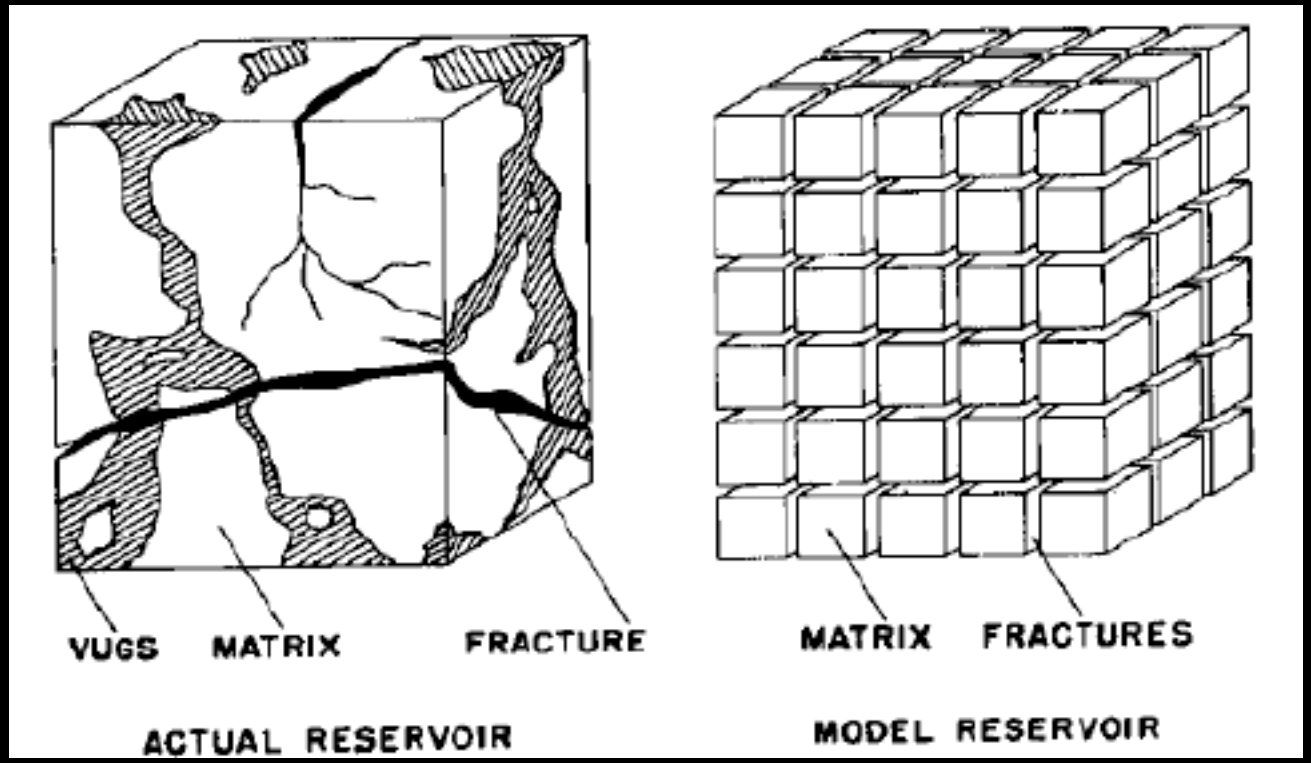

Double porosity

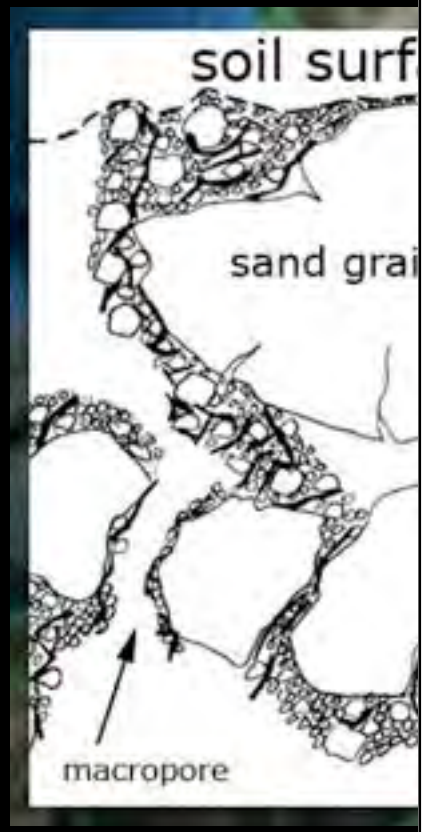

Double porosity

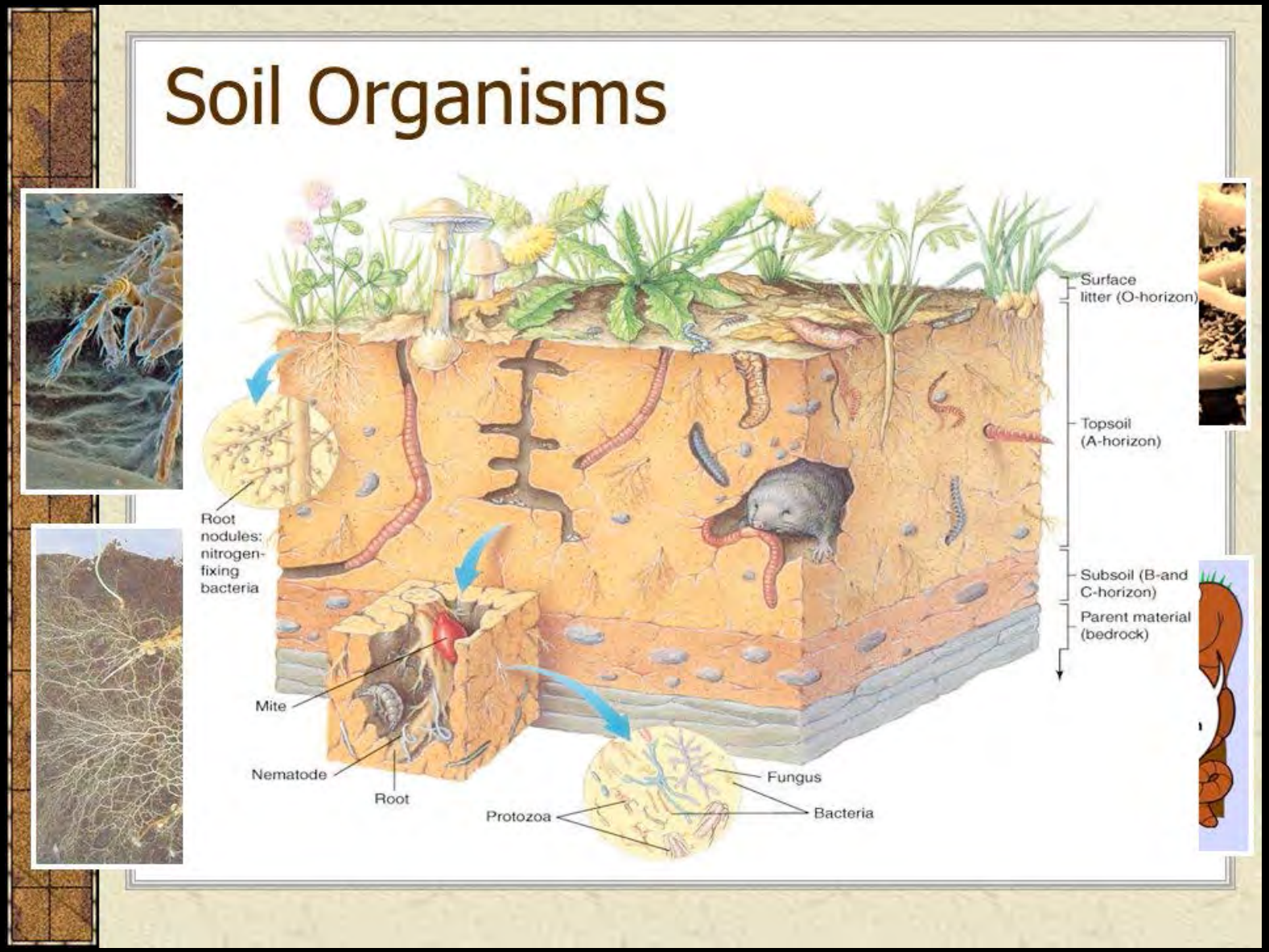

Double porosity

Aggregated Bioley silt (Koliji, Vulliet & Laloui 2010)

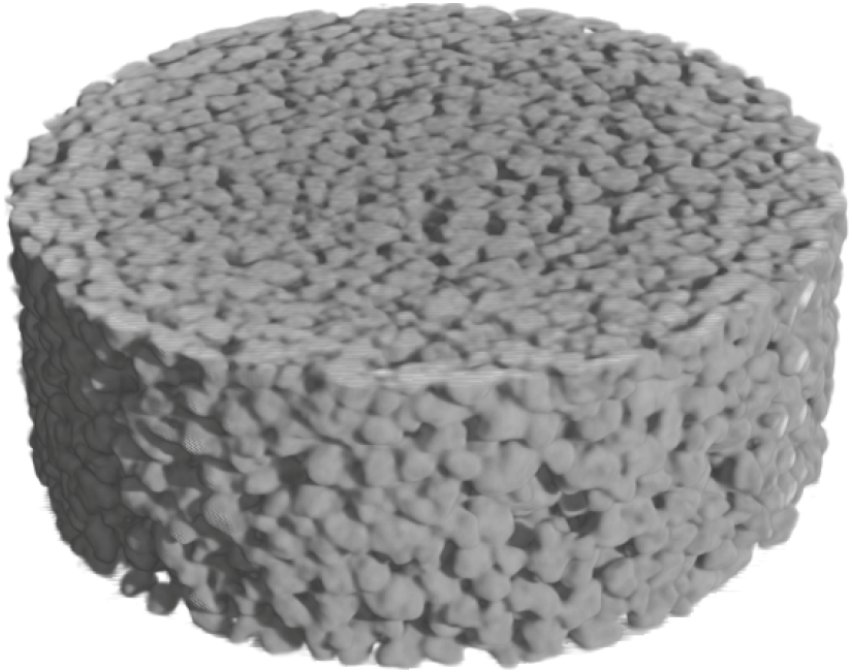

neutron tomography

Double porosity

Aggregated Bioley silt (Koliji, Vulliet & Laloui 2010)

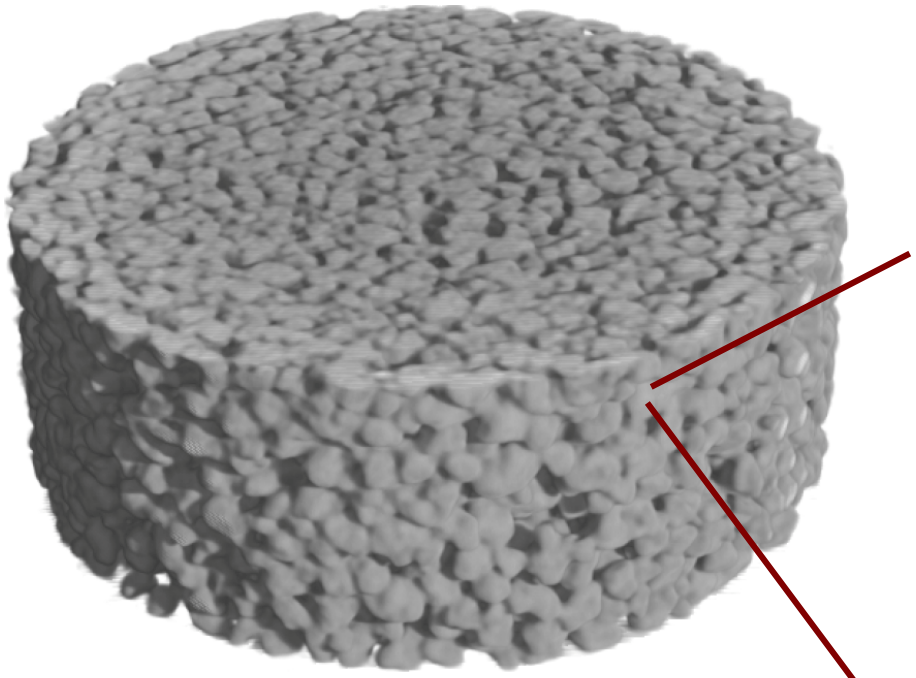

neutron tomography

ESEM

Double porosity

Aggregated Bioley silt (Koliji, Vulliet & Laloui 2010)

- macropores
- micropores

- dual porosity
- dual permeability

Double porosity

Aggregated Bioley silt (Koliji, Vulliet & Laloui 2010)

- macropores
- micropores

double porosity

- dual porosity
- dual permeability

Double porosity

Mechanisms considered

- Flow through the micropores
- Flow through the macropores
- Fluid mass exchange between the micropores and macropores

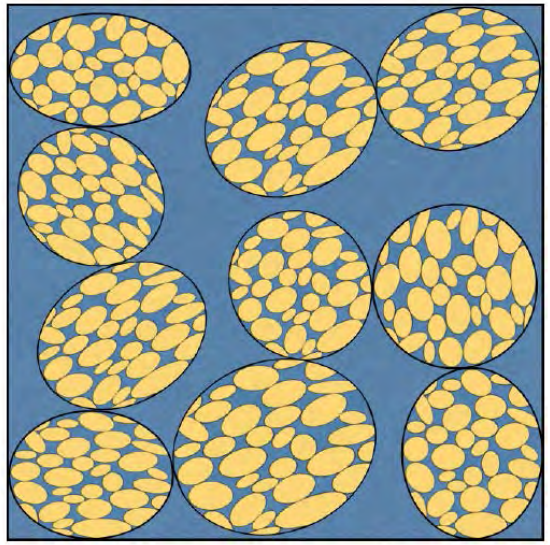

Double porosity

Mechanisms considered

- Flow through the micropores
- Flow through the macropores
- Fluid mass exchange between the micropores and macropores

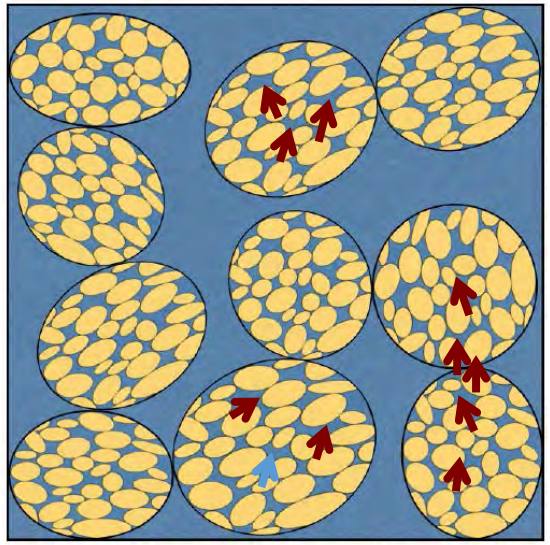

Double porosity

Mechanisms considered

- Flow through the micropores
- Flow through the macropores
- Fluid mass exchange between the micropores and macropores

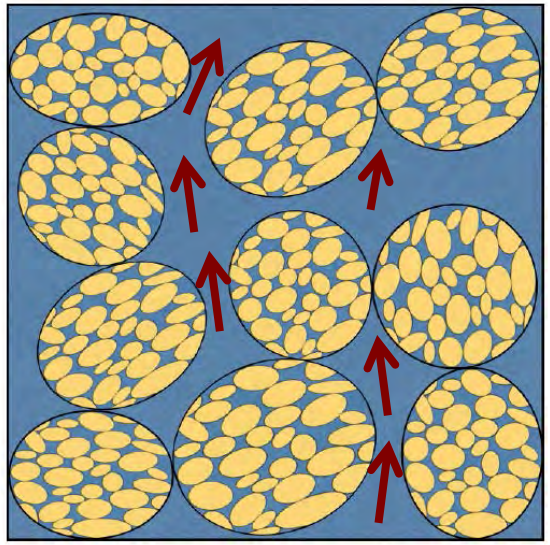

Double porosity

Mechanisms considered

- Flow through the micropores
- Flow through the macropores
- Fluid mass exchange between the micropores and macropores

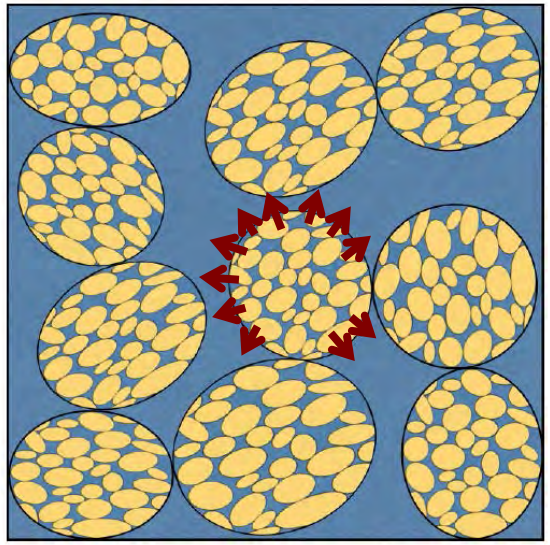

Double porosity

Aggregated Bioley silt (Koliji, Vulliet & Laloui 2008)

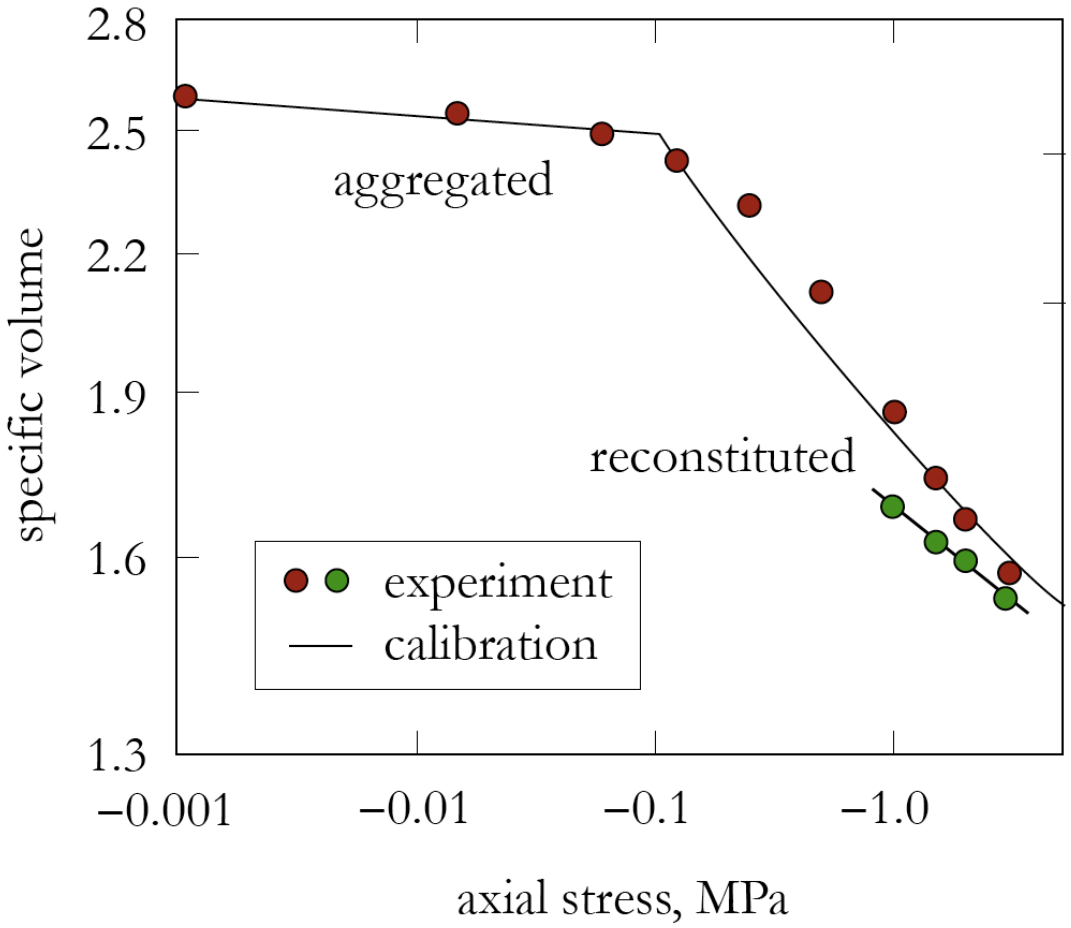

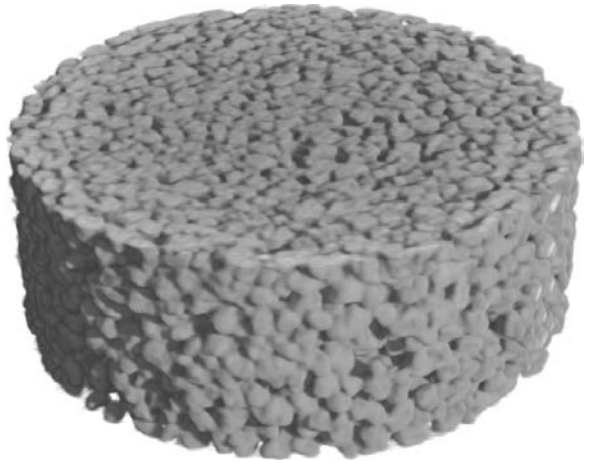

Double porosity

Cubzak-Les-Ponts clay (Cosenza & Korosak 2014)

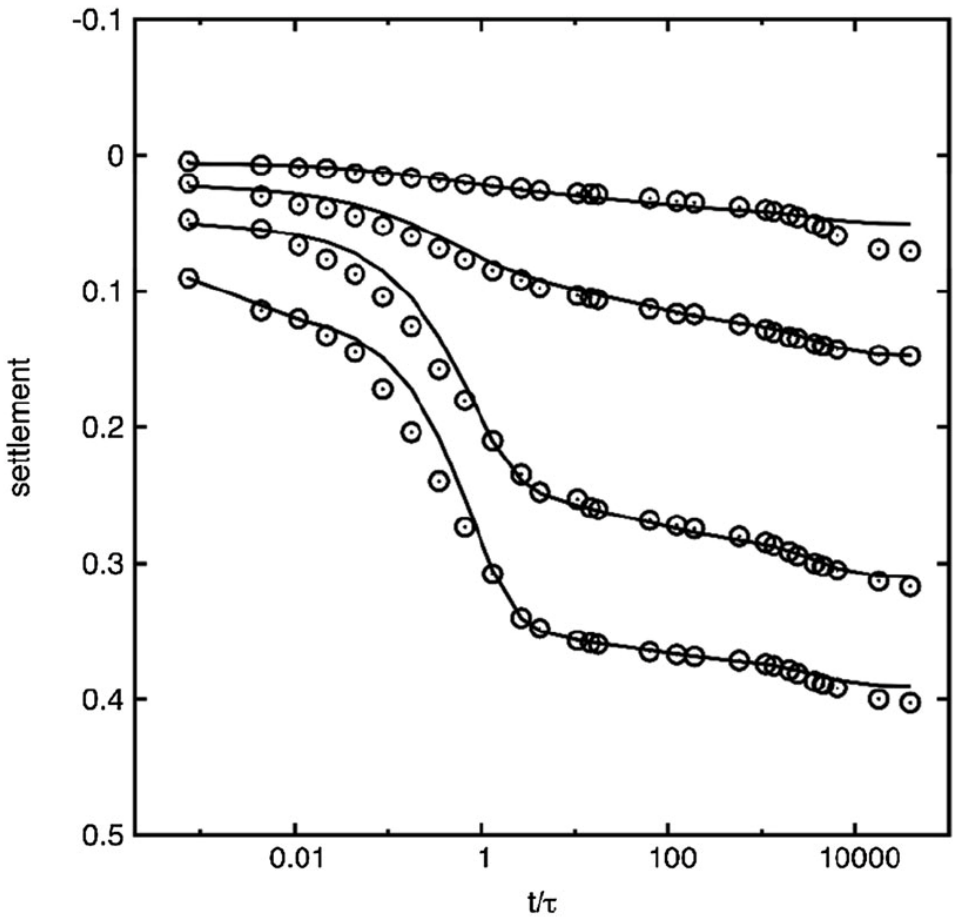

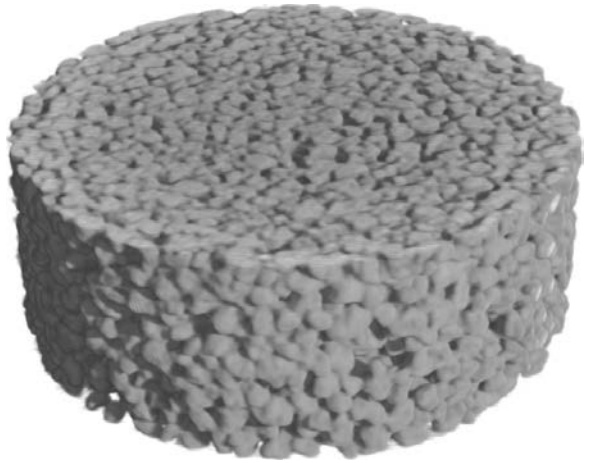

Effective stress equation (Borja & Koliji, JMPS, 2009)

$$\boldsymbol{\sigma}' = \boldsymbol{\sigma} + B\bar{p}\mathbf{1}$$

$$\bar{p} = \sum_{i=M,m} \left[\psi^i S^i p_i + \psi^i (1 - S^i) p_{ia}\right]$$

Overall mean pore pressure:

- For each pore scale, take the weighted sum of the pore air and pore water pressures with the local saturations taken as the weights.
- Take the sum of the mean pore pressures at each pore scale with the pore fractions taken as the weights.

Effective stress equation (Borja & Koliji, JMPS, 2009)

$$\boldsymbol{\sigma}' = \boldsymbol{\sigma} + B\bar{p}\mathbf{1}$$

$$\bar{p} = \sum_{i=M,m} \left[\psi^i S^i p_i + \psi^i (1 - S^i) p_{ia}\right]$$

1.0

0

Overall mean pore pressure:

- For fully saturated media, take the weighted sum of the pore pressures with the pore fractions taken as the weights.
- Need a finite deformation formulation to track the evolution of the ore fractions.

Volume relationships:

- Void ratios

$$e_m(\boldsymbol{X},t) = \frac{\mathrm{d}V_{vm}}{\mathrm{d}V_s}\,, \qquad e_M(\boldsymbol{X},t) = \frac{\mathrm{d}V_{vM}}{\mathrm{d}V_s}$$

- Volume fractions

$$\phi^s(\boldsymbol{X},t) = \frac{\mathrm{d}V_s}{\mathrm{d}V}\,, \qquad \psi(\boldsymbol{X},t) = \frac{\mathrm{d}V_{vm}}{\mathrm{d}V_v}$$

- Specific volumes

$$v_m(\boldsymbol{X},t) = 1 + e_m(\boldsymbol{X},t)$$

$$v(\boldsymbol{X},t) = v_m(\boldsymbol{X},t) + e_M(\boldsymbol{X},t)$$

Conservation laws

Balance of linear momentum

$$\mathrm{DIV}(\boldsymbol{P}) + \rho_0 \boldsymbol{G} = c_0(\tilde{\boldsymbol{v}}_m - \tilde{\boldsymbol{v}}_M)$$

Balance of fluid mass

$$\dot{\rho}_0^M + \mathrm{DIV}(\boldsymbol{Q}_M) = -c_0$$
$$\dot{\rho}_0^m + \mathrm{DIV}(\boldsymbol{Q}_m) = c_0$$

- subject to boundary and initial conditions

Internal energy equation

$$J\rho\dot{e} = \langle \bar{\boldsymbol{\tau}}, \boldsymbol{d} \rangle + \sum_{i=M,m} \langle \tilde{\boldsymbol{v}}_i, \phi^i, p_i \rangle - \sum_{i=M,m} \langle c^i, p_i, \tilde{\boldsymbol{v}}_i \rangle - \langle (1-\phi^s), \pi, \dot{\psi} \rangle$$

Internal energy equation

$$J\rho\dot{e} = \langle \bar{\boldsymbol{\tau}}, \boldsymbol{d} \rangle + \sum_{i=M,m} \langle \tilde{\boldsymbol{v}}_i, \phi^i, p_i \rangle - \sum_{i=M,m} \langle c^i, p_i, \tilde{\boldsymbol{v}}_i \rangle - \langle (1-\phi^s), \pi, \dot{\psi} \rangle$$

- Mechanical constitutive law in terms of effective stress – modified Cam-Clay

Internal energy equation

$$J\rho\dot{e} = \langle \bar{\boldsymbol{\tau}}, \boldsymbol{d} \rangle + \boxed{\sum_{i=M,m} \langle \tilde{\boldsymbol{v}}_i, \phi^i, p_i \rangle} - \sum_{i=M,m} \langle c^i, p_i, \tilde{\boldsymbol{v}}_i \rangle - \langle (1-\phi^s), \pi, \dot{\psi} \rangle$$

- Darcy's law at each pore scale

Internal energy equation

$$J\rho\dot{e} = \langle \bar{\boldsymbol{\tau}}, \boldsymbol{d} \rangle + \sum_{i=M,m} \langle \tilde{\boldsymbol{v}}_i, \phi^i, p_i \rangle - \boxed{\sum_{i=M,m} \langle c^i, p_i, \tilde{\boldsymbol{v}}_i \rangle} - \langle (1-\phi^s), \pi, \dot{\psi} \rangle$$

- Mass transfer law (Gerke and Van Genuchten 1993)

$$c = \frac{\bar{\alpha}}{\mu_w}(p_M - p_m)$$

Internal energy equation

$$J\rho\dot{e} = \langle \bar{\boldsymbol{\tau}}, \boldsymbol{d} \rangle + \sum_{i=M,m} \langle \tilde{\boldsymbol{v}}_i, \phi^i, p_i \rangle - \sum_{i=M,m} \langle c^i, p_i, \tilde{\boldsymbol{v}}_i \rangle - \boxed{\langle (1-\phi^s), \pi, \dot{\psi} \rangle}$$

- Evolution of the micropore fraction

  $\pi = p_{cM} - p_{cm}$

Model validation

Corinth marl
(Anagnostopolous et al. 1991)

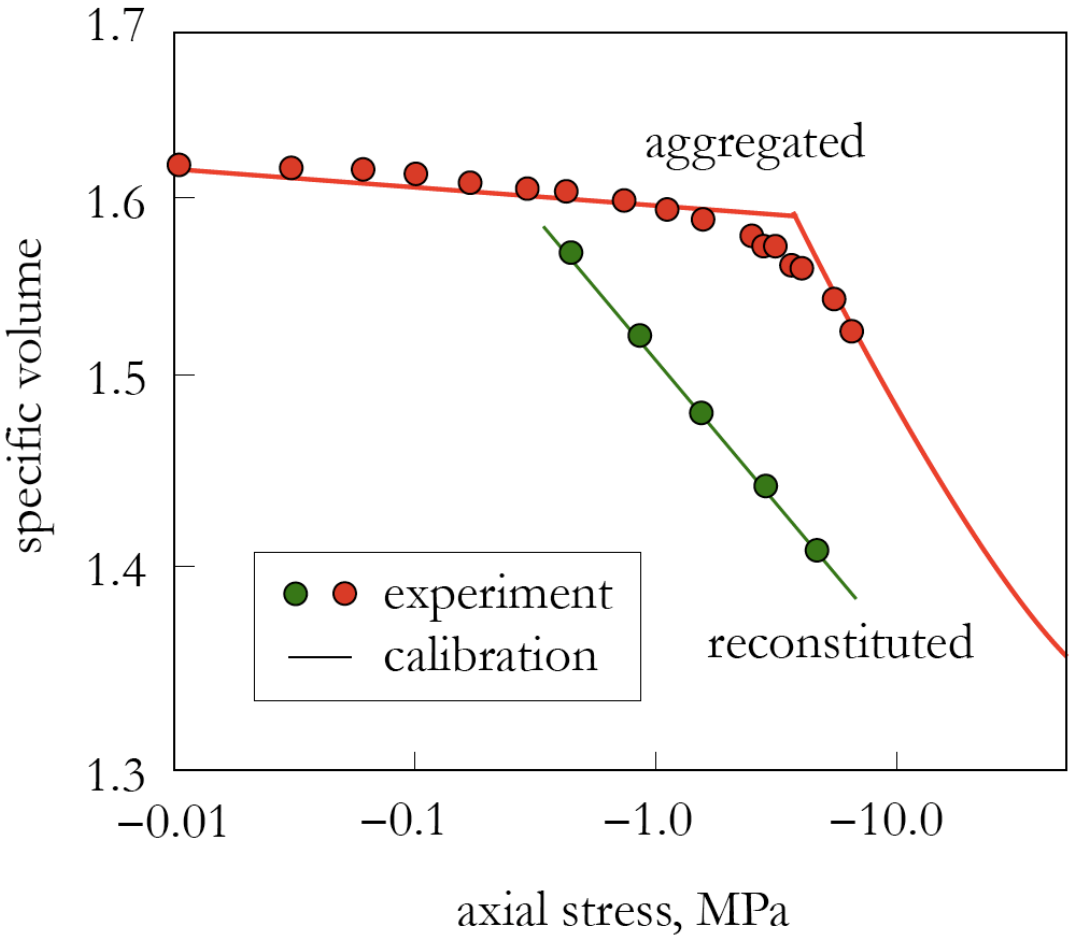

Model validation

Corinth marl
(Anagnostopolous et al. 1991)

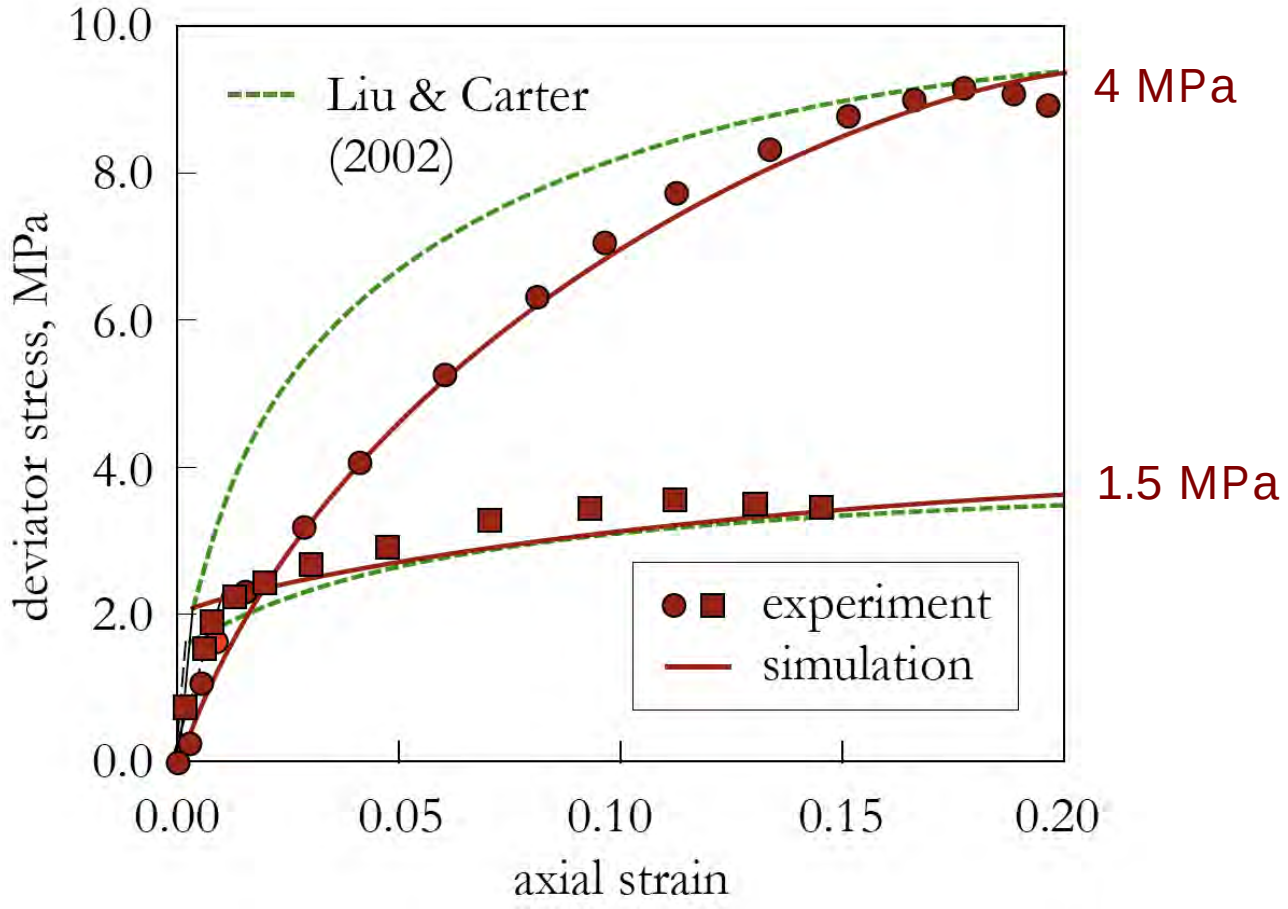

Model validation

Corinth marl
(Anagnostopolous et al. 1991)

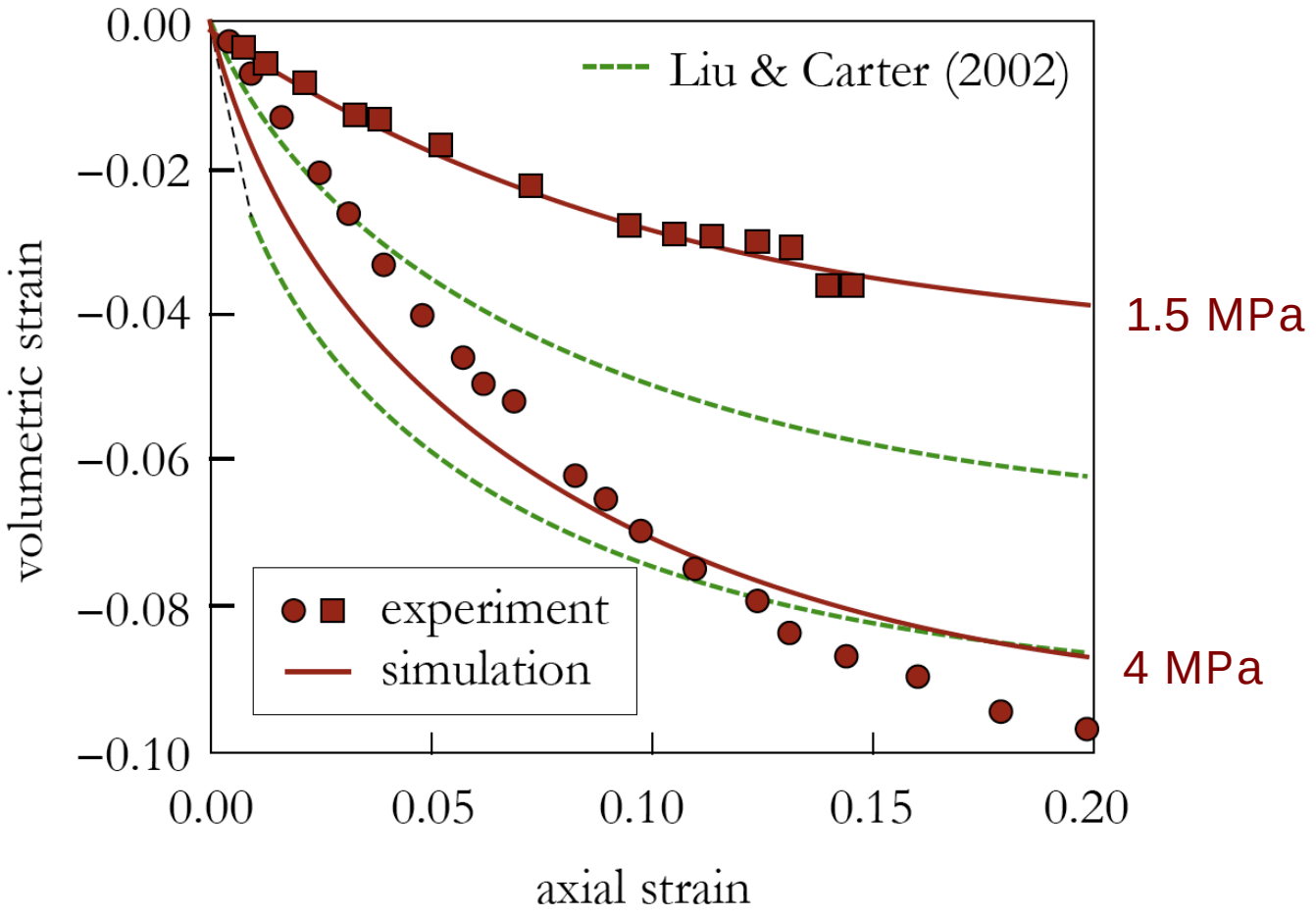

One-dimensional consolidation

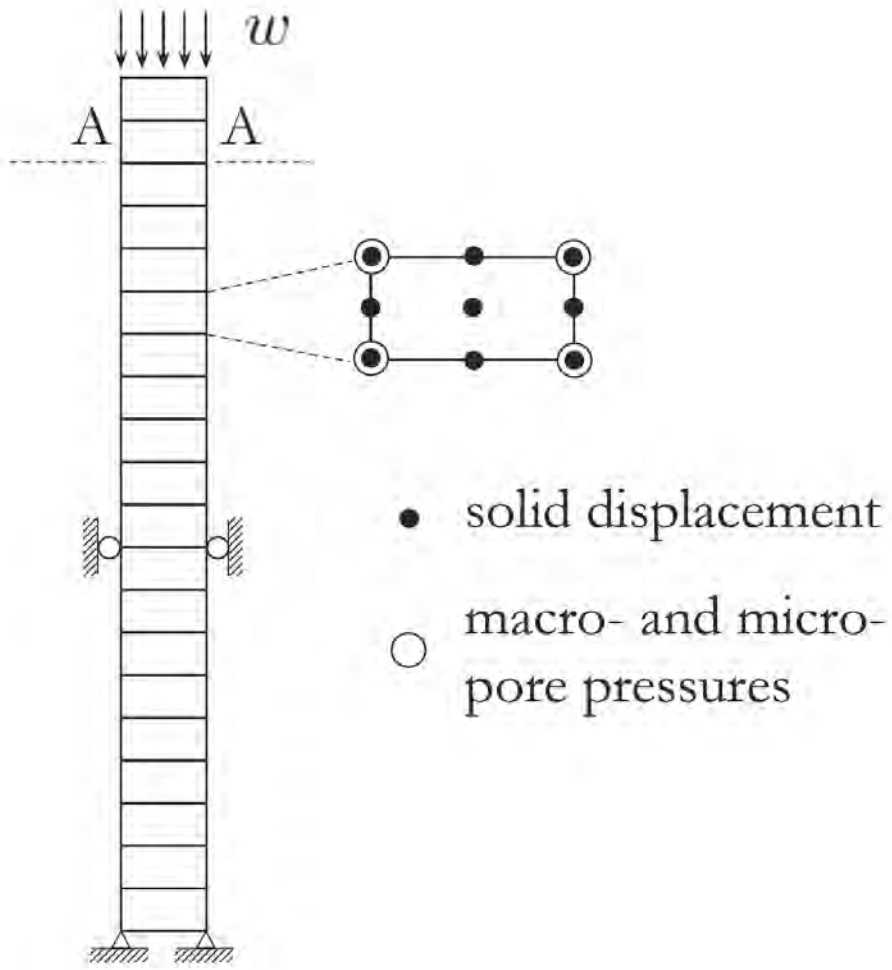

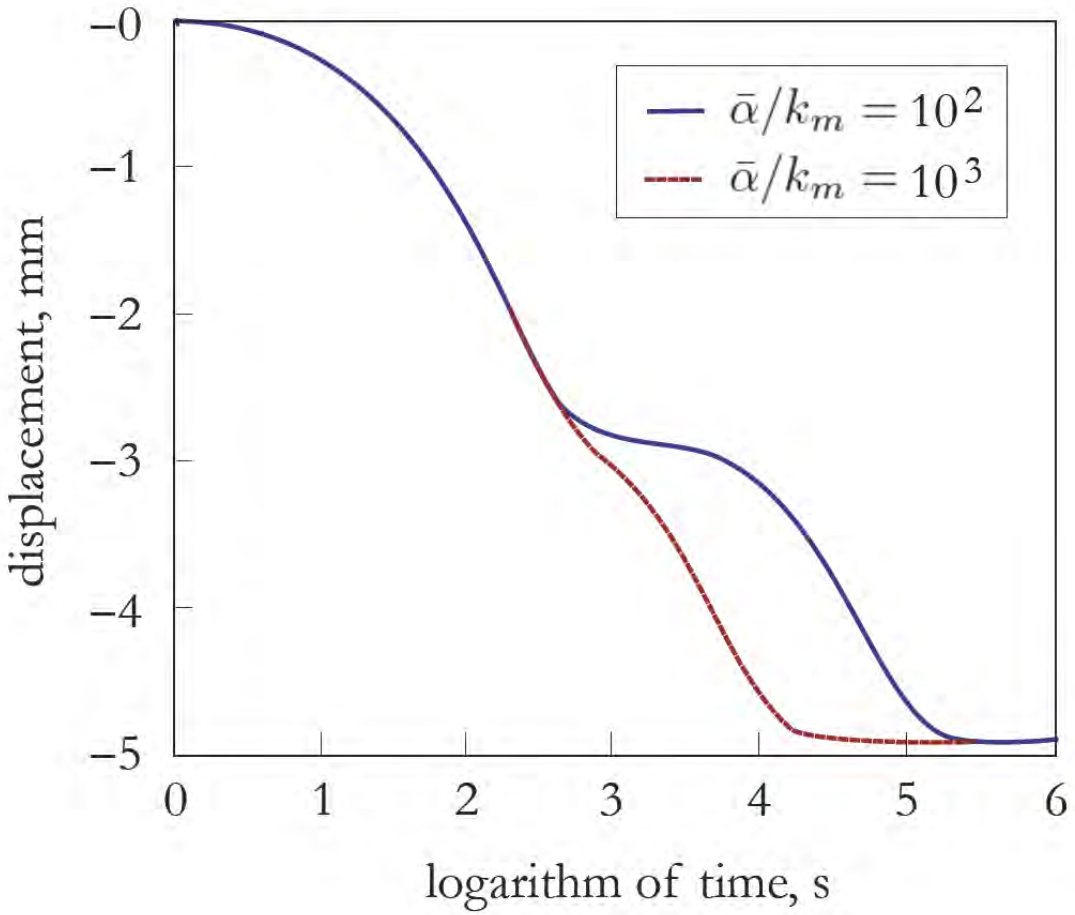

Geomaterials are crucial in many engineering applications

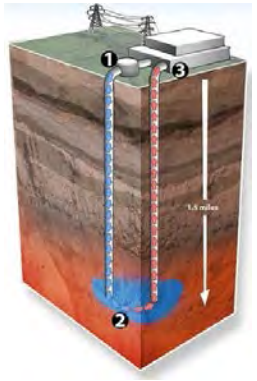

Geothermal energy

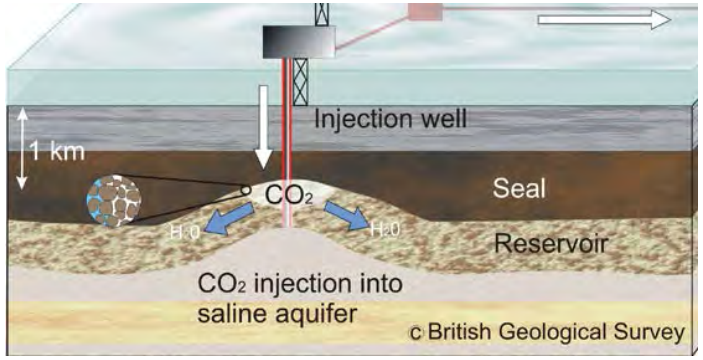

Carbon sequestration

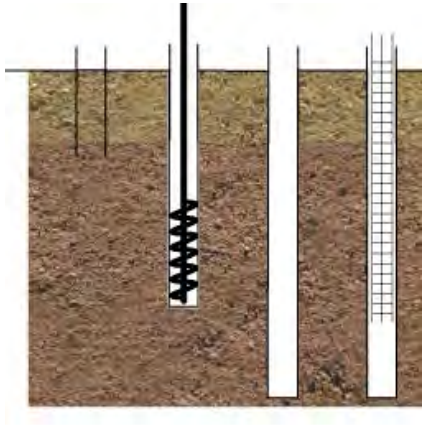

Wellbore drilling

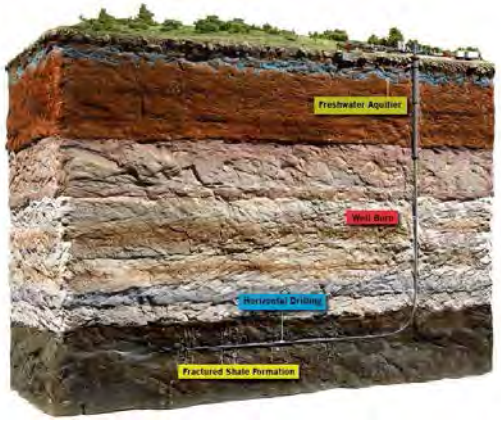

Hydraulic fracturing

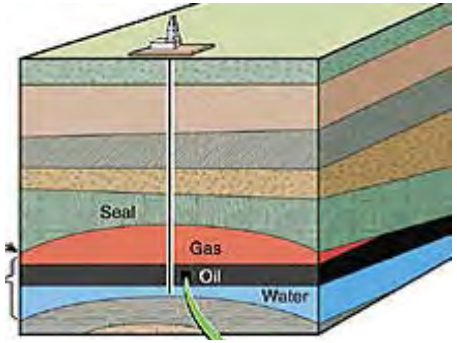

Hydrocarbon recovery

Waste storage

Motivations – transversely isotropic rocks

These applications involve various multiphysics processes

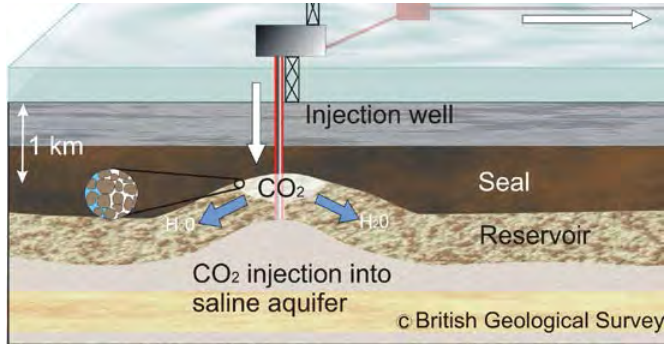

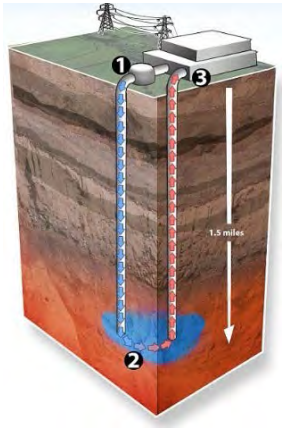

Multiphysics processes:

- Solid deformation
- Instability/fracture/failure
- Temperature
- Fluid flow
- Chemical reactions
- …

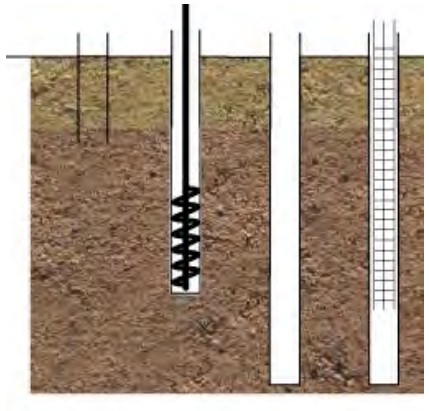

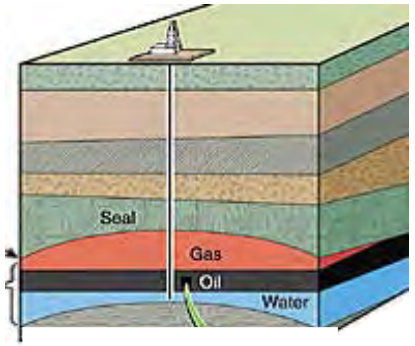

Anisotropy

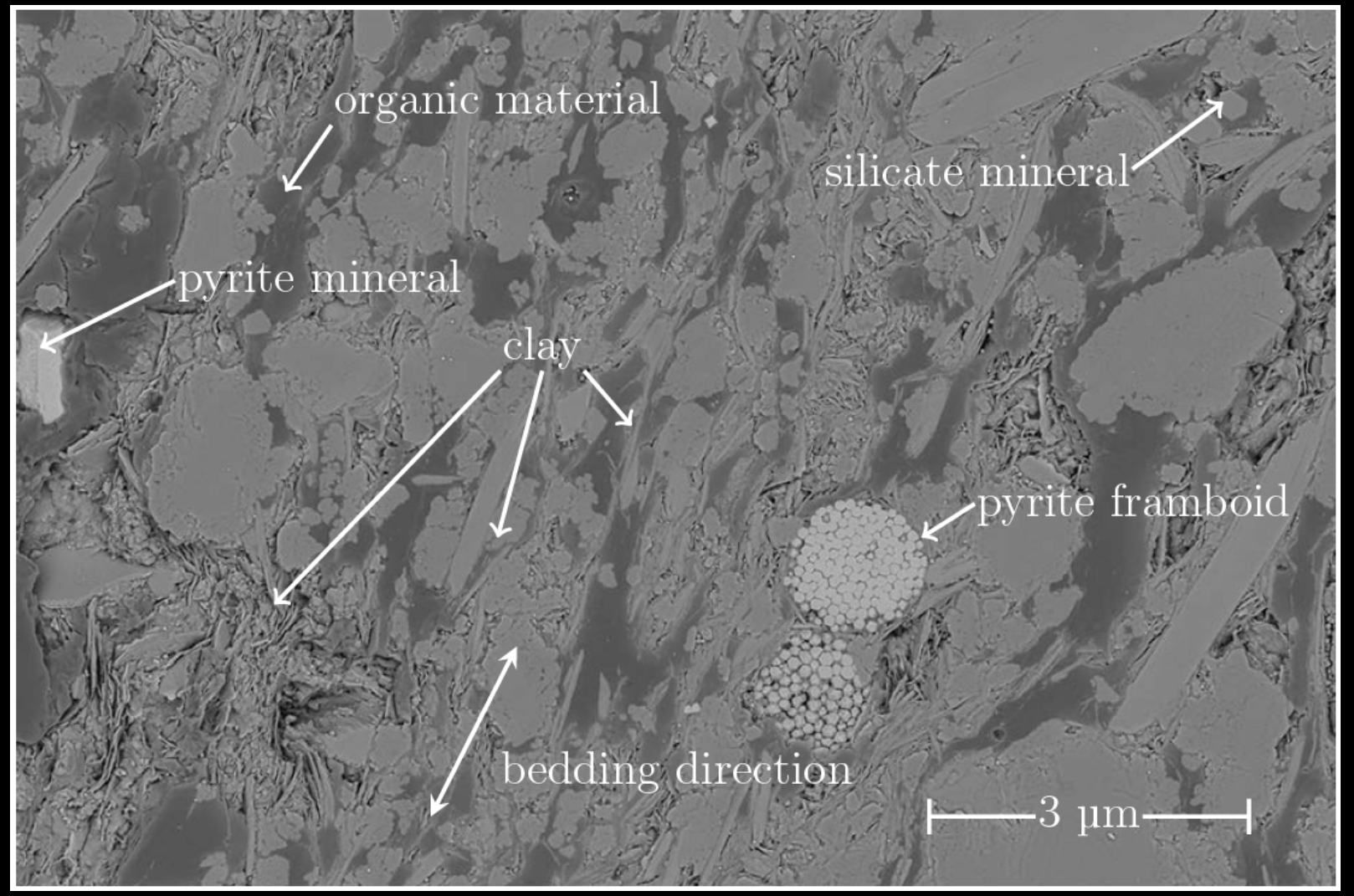

FIB-SEM, Woodford Shale

Bennett et al. (2015)

Anisotropy

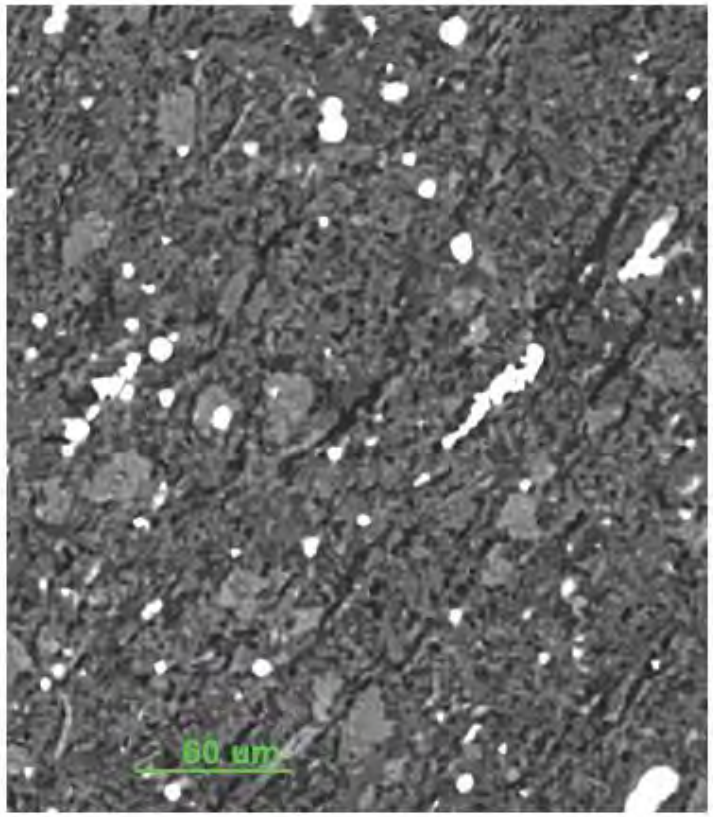

(a)

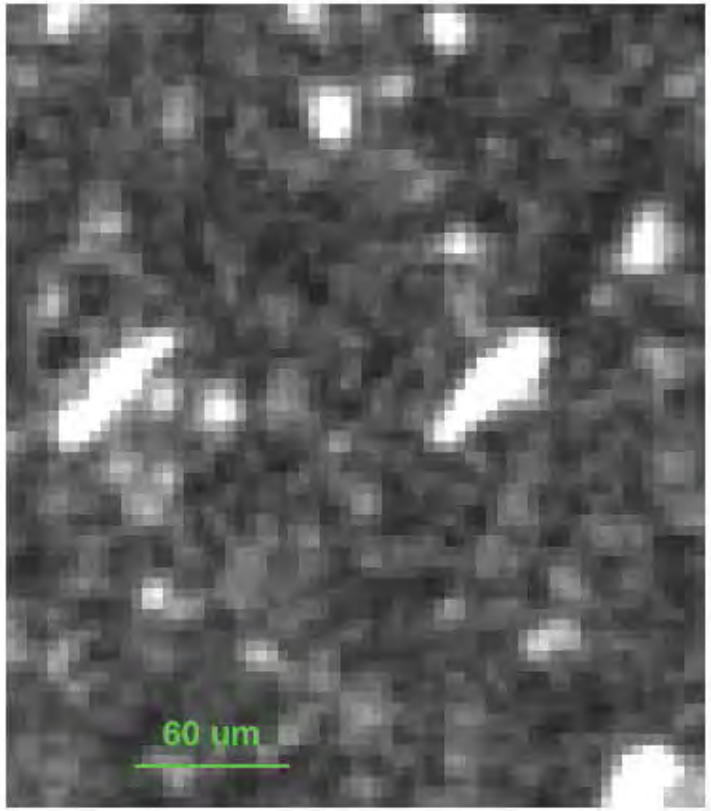

(b)

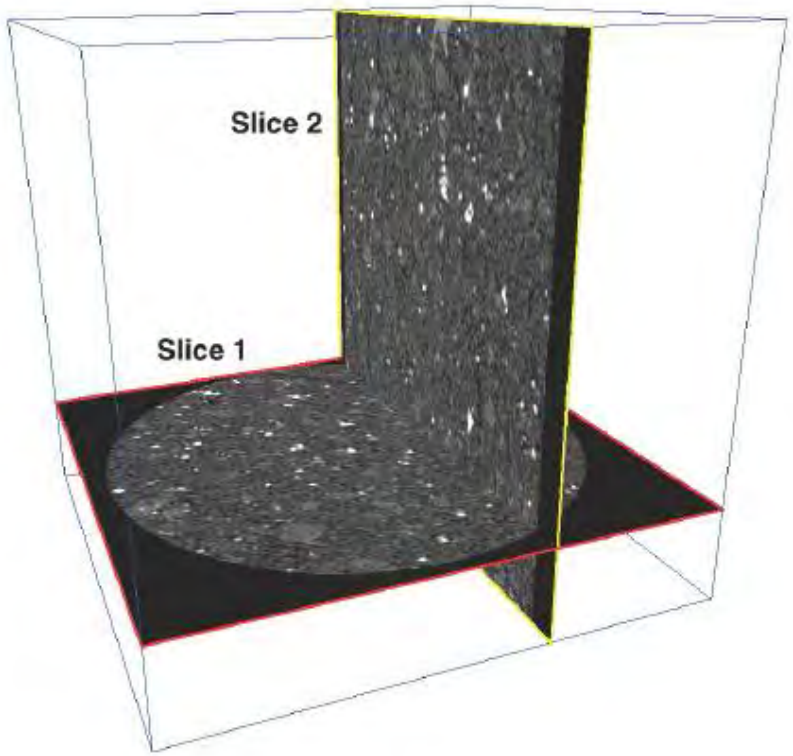

(c)

Micro-CT, Woodford Shale

Semnani et al. (2016)

Evidence of anisotropy in the laboratory

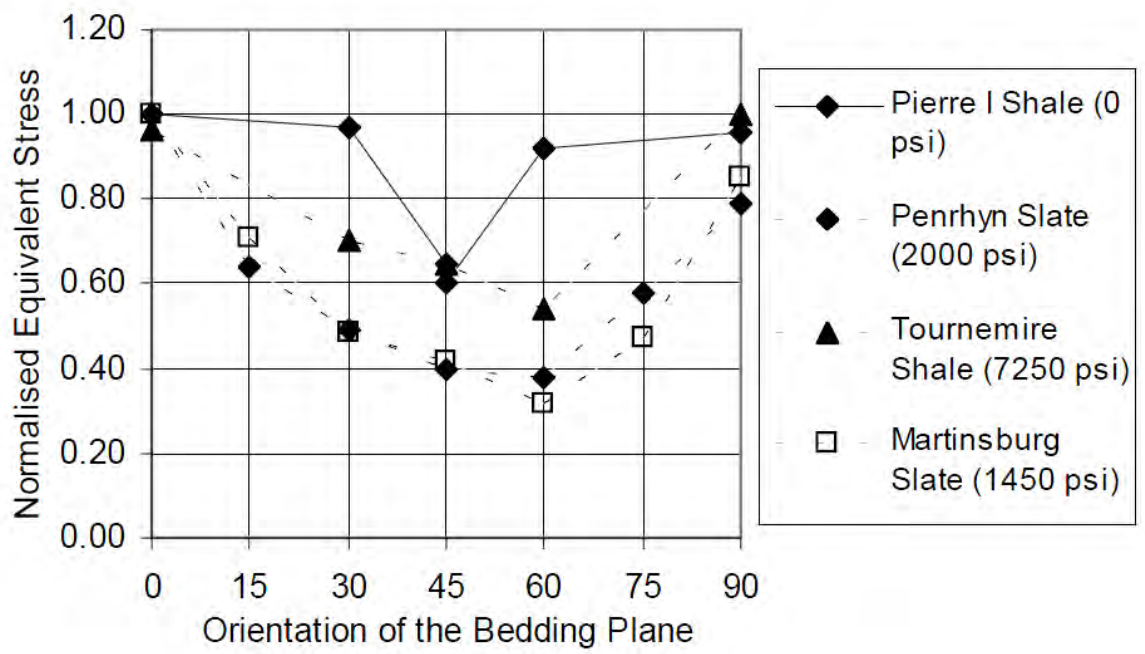

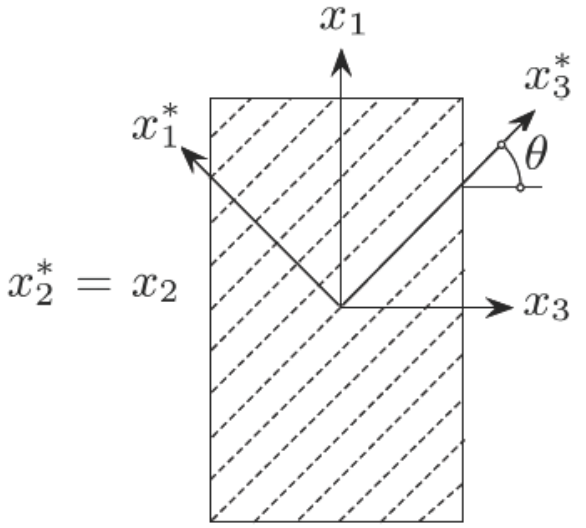

Variation of the compressive strength with orientation of bedding plane (After Crook et al., 2002)

Transverse isotropy

- Material symmetry group

$$\mathcal{G} = \{\boldsymbol{Q} \mid \boldsymbol{Q} \cdot \boldsymbol{l}_1 = \boldsymbol{l}_1\}$$

- Microstructure tensor

$$\boldsymbol{\phi} = \boldsymbol{l}_1 \otimes \boldsymbol{l}_1$$

- Transverse isotropy

$$\boldsymbol{Q} \cdot \boldsymbol{\phi} \cdot \boldsymbol{Q}^{\mathsf{T}} = \boldsymbol{\phi} \qquad \forall\, \boldsymbol{Q} \in \mathcal{G}$$

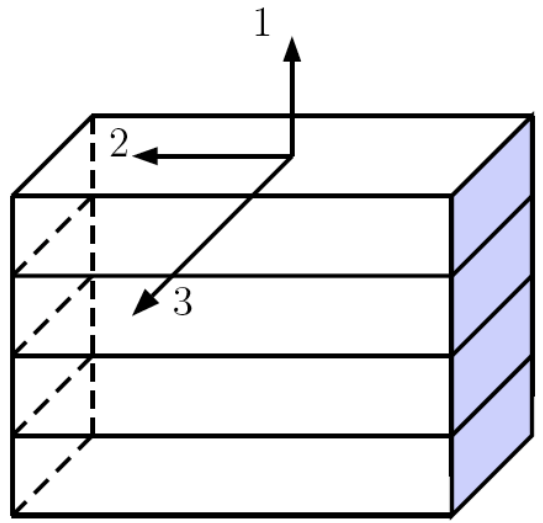

Compliance matrix for linear elasticity (5 constants):

$$[\boldsymbol{C}^e]^{-1} = \begin{bmatrix} 1/E_1 & -\nu_{12}/E_2 & \nu_{12}/E_2 & 0 & 0 & 0 \\ -\nu_{12}/E_2 & 1/E_2 & -\nu_{23}/E_2 & 0 & 0 & 0 \\ -\nu_{12}/E_2 & -\nu_{23}/E_2 & 1/E_2 & 0 & 0 & 0 \\ 0 & 0 & 0 & 0.5/G_{23} & 0 & 0 \\ 0 & 0 & 0 & 0 & 0.5/G_{12} & 0 \\ 0 & 0 & 0 & 0 & 0 & 0.5/G_{12} \end{bmatrix}$$

Compliance matrix for linear elasticity (5 constants):

$$[C^e]^{-1} = \begin{bmatrix} 1/E_1 & -\nu_{12}/E_2 & \nu_{12}/E_2 & 0 & 0 & 0 \\ -\nu_{12}/E_2 & 1/E_2 & -\nu_{23}/E_2 & 0 & 0 & 0 \\ -\nu_{12}/E_2 & -\nu_{23}/E_2 & 1/E_2 & 0 & 0 & 0 \\ 0 & 0 & 0 & 0.5/G_{23} & 0 & 0 \\ 0 & 0 & 0 & 0 & 0.5/G_{12} & 0 \\ 0 & 0 & 0 & 0 & 0 & 0.5/G_{12} \end{bmatrix}$$

not linearly independent

Implications of transverse isotropy

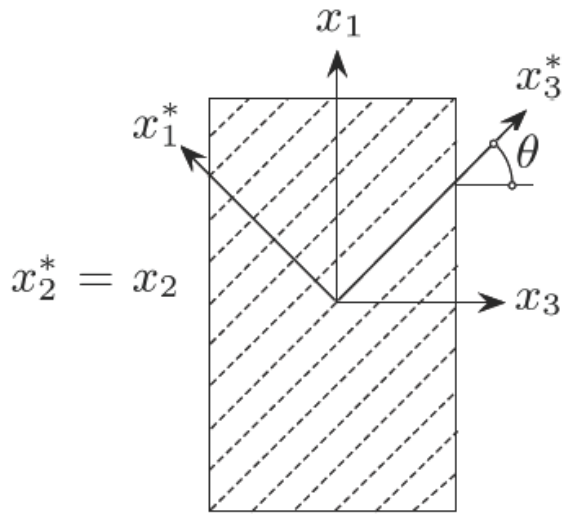

Schematics

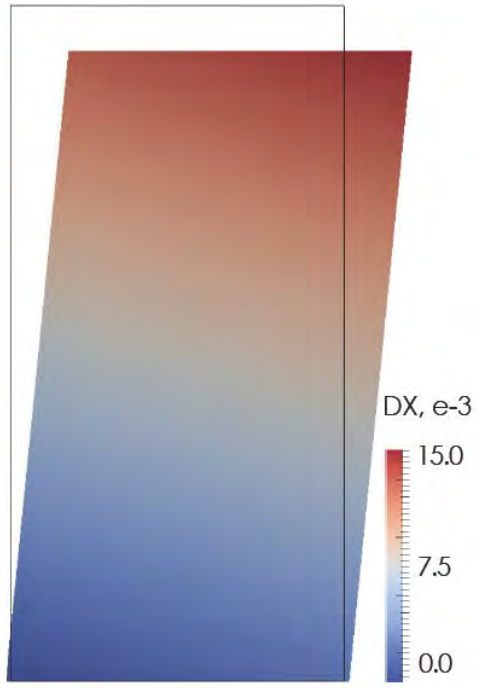

theta = 45º

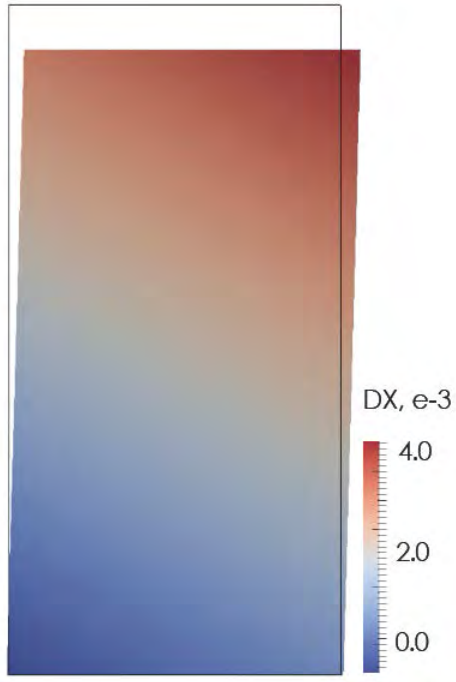

theta = 15º

- Alternative stress tensor

$$\boldsymbol{\sigma}^* = \mathbb{P} : \boldsymbol{\sigma}$$

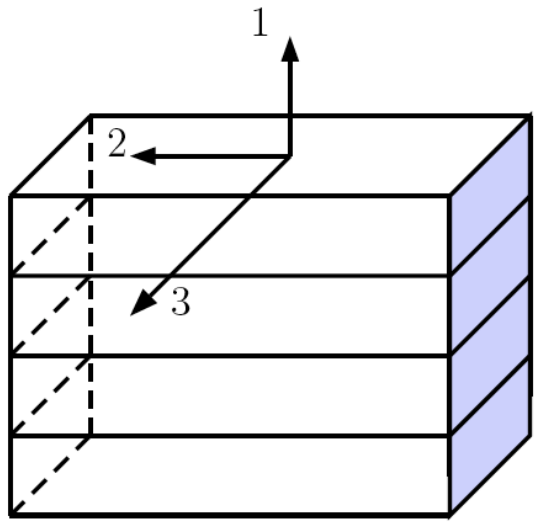

- Projection tensor

$$\begin{aligned}\mathbb{P}_{ijkl} =& \frac{c_1}{2}\left(\delta_{ik}\delta_{jl} + \delta_{il}\delta_{jk}\right) \\ &+ \frac{c_2}{2}\left(\phi_{ik}\phi_{jl} + \phi_{il}\phi_{jk}\right) \\ &+ \frac{c_3}{4}\left(\delta_{ik}\phi_{jl} + \delta_{il}\phi_{jk} + \phi_{ik}\delta_{jl} + \phi_{il}\delta_{jk}\right)\end{aligned}$$

Semnani et al. (2016)

- Alternative stress tensor

$$\boldsymbol{\sigma}^* = \mathbb{P} : \boldsymbol{\sigma}$$

- Coordinate axes aligned with bedding planes:

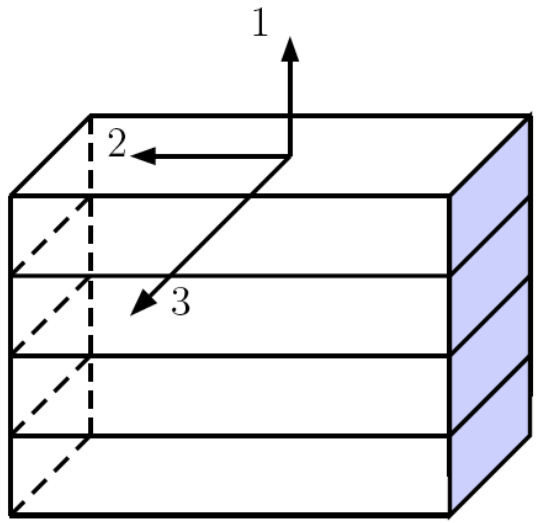

$$\begin{Bmatrix} \sigma^*_{11} \\ \sigma^*_{22} \\ \sigma^*_{33} \\ \sigma^*_{23} \\ \sigma^*_{13} \\ \sigma^*_{12} \end{Bmatrix} = \begin{bmatrix} \alpha & & & & & \\ & \beta & & & & \\ & & \beta & & & \\ & & & \beta & & \\ & & & & \gamma & \\ & & & & & \gamma \end{bmatrix} \begin{Bmatrix} \sigma_{11} \\ \sigma_{22} \\ \sigma_{33} \\ \sigma_{23} \\ \sigma_{13} \\ \sigma_{12} \end{Bmatrix}$$

Semnani et al. (2016)

- Alternative stress tensor

$$\boldsymbol{\sigma}^* = \mathbb{P} : \boldsymbol{\sigma}$$

- Coordinate axes aligned with bedding planes:

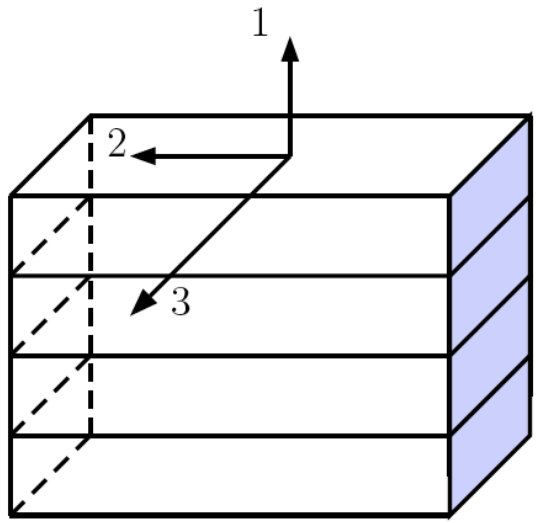

$$\begin{Bmatrix} \sigma^*_{11} \\ \sigma^*_{22} \\ \sigma^*_{33} \\ \sigma^*_{23} \\ \sigma^*_{13} \\ \sigma^*_{12} \end{Bmatrix} = \begin{bmatrix} \alpha & & & & & \\ & \beta & & & & \\ & & \beta & & & \\ & & & \beta & & \\ & & & & \gamma & \\ & & & & & \gamma \end{bmatrix} \begin{Bmatrix} \sigma_{11} \\ \sigma_{22} \\ \sigma_{33} \\ \sigma_{23} \\ \sigma_{13} \\ \sigma_{12} \end{Bmatrix}$$

1.0

1.0

Semnani et al. (2016)

- Yield function

$$f(\boldsymbol{\sigma}) = f_{iso}(\boldsymbol{\sigma}^*)$$

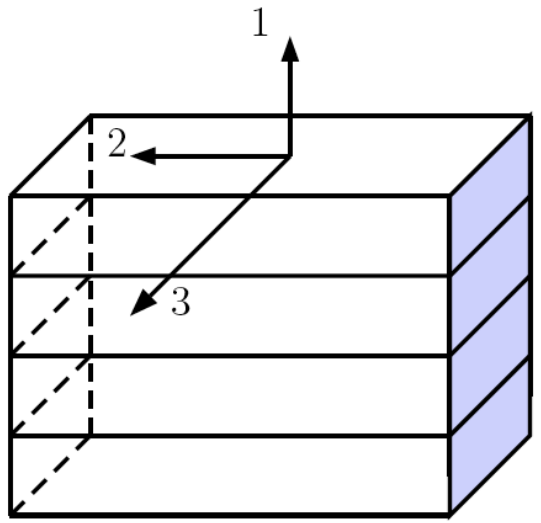

- Alternative stress configuration:

$$f(\boldsymbol{\sigma}) = \frac{q^{*2}}{M^2} + p^*(p^* - p_c) \leq 0$$

- Real stress configuration:

$$f(\boldsymbol{\sigma}) = \frac{\|\boldsymbol{\sigma}\|^2_{\mathbb{A}^*}}{2M^2} + (\boldsymbol{a}^* : \boldsymbol{\sigma})(\boldsymbol{a}^* : \boldsymbol{\sigma} - p_c) \leq 0$$

Semnani et al. (2016)

Yield surfaces

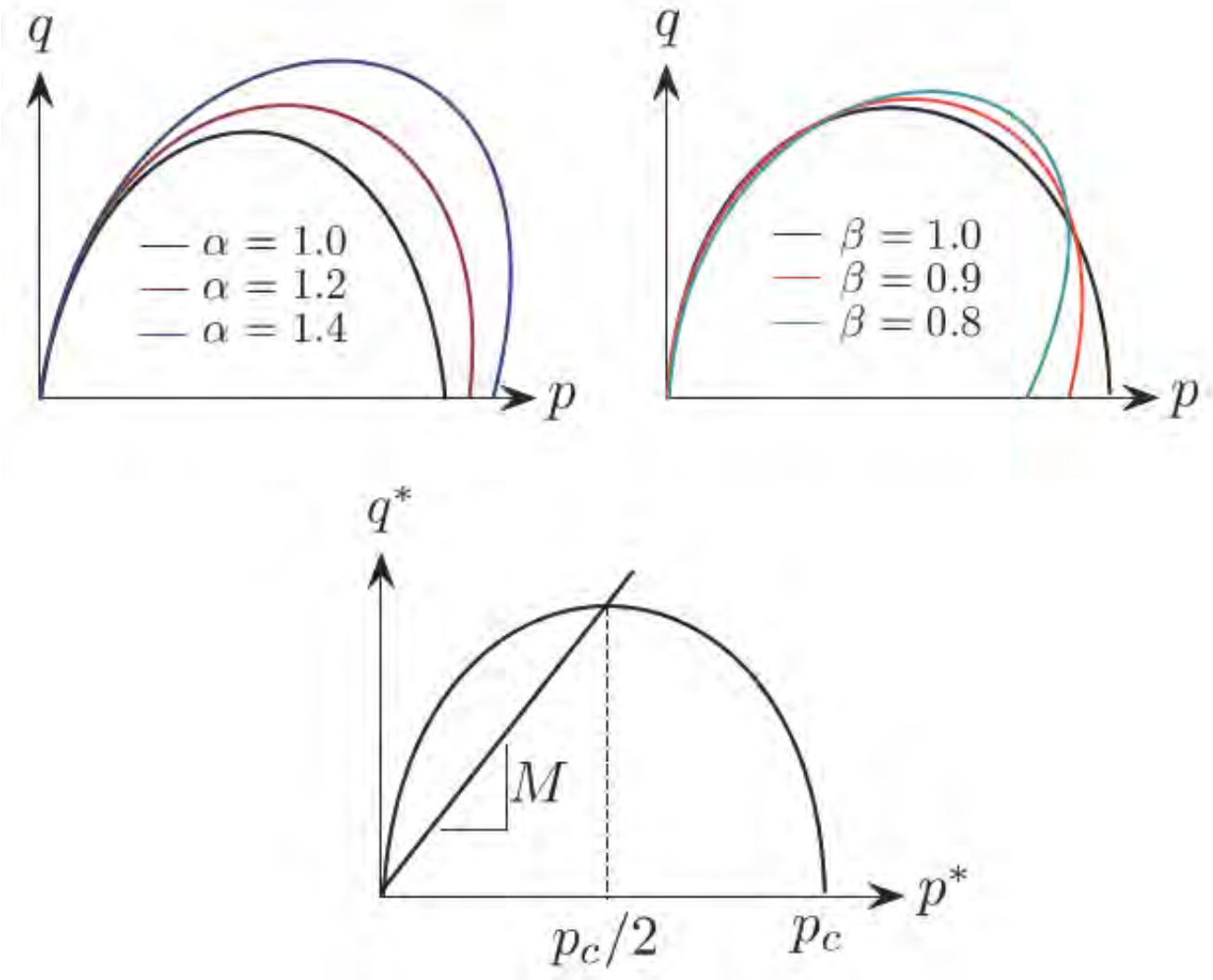

Semnani et al. (2016)

- Flow rule

$$\dot{\boldsymbol{\epsilon}}^p = \dot{\lambda}\frac{\partial f}{\partial \boldsymbol{\sigma}} = \dot{\lambda}\frac{\partial f_{iso}}{\partial \boldsymbol{\sigma}^*} : \frac{\partial \boldsymbol{\sigma}^*}{\partial \boldsymbol{\sigma}} = \dot{\lambda}\mathbb{P} : \frac{\partial f_{iso}}{\partial \boldsymbol{\sigma}^*}$$

- Laloui and Cekerevac (2003) softening law:

$$p_c = p_{c0} \exp\left(\frac{\epsilon_v^p}{\lambda^p}\right) \mathscr{G}\left(\Theta\right)$$

$$\mathscr{G}\left(\Theta\right) = \left[1 - \gamma_T \ln\left(1 + \frac{\Delta\Theta}{\Theta_0 - 273}\right)\right]$$

Semnani et al. (2016)

Anisotropic thermoplasticity

- Rate equation $\dot{\boldsymbol{\sigma}} = \mathbb{C}^{ep} : \dot{\boldsymbol{\epsilon}} + \boldsymbol{\tau}\dot{\Theta}$
- Isothermal condition $\dot{\boldsymbol{\sigma}} = \mathbb{C}^{ep} : \dot{\boldsymbol{\epsilon}}$
- Adiabatic condition $\rho c\dot{\Theta} = \zeta \boldsymbol{\sigma} : \dot{\boldsymbol{\epsilon}}^{p}$

  $\dot{\boldsymbol{\sigma}} = \mathbb{C}^{ept} : \dot{\boldsymbol{\epsilon}}$
- Shear band analysis: Rudnicki and Rice (1975) criterion

Semnani et al. (2016)

TX compression of NC Tournemire shale

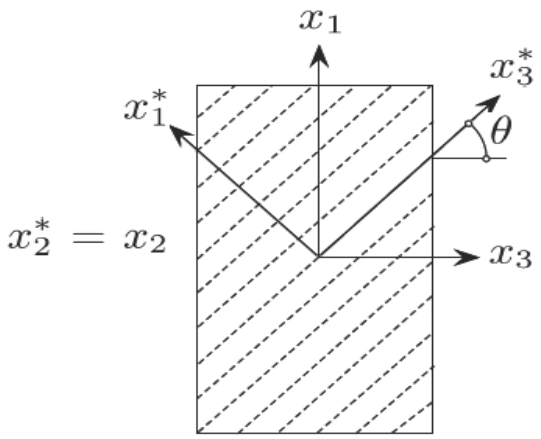

- Isothermal and adiabatic, at theta = 45º and 40 MPa confining pressure, Zhao et al. (2018)

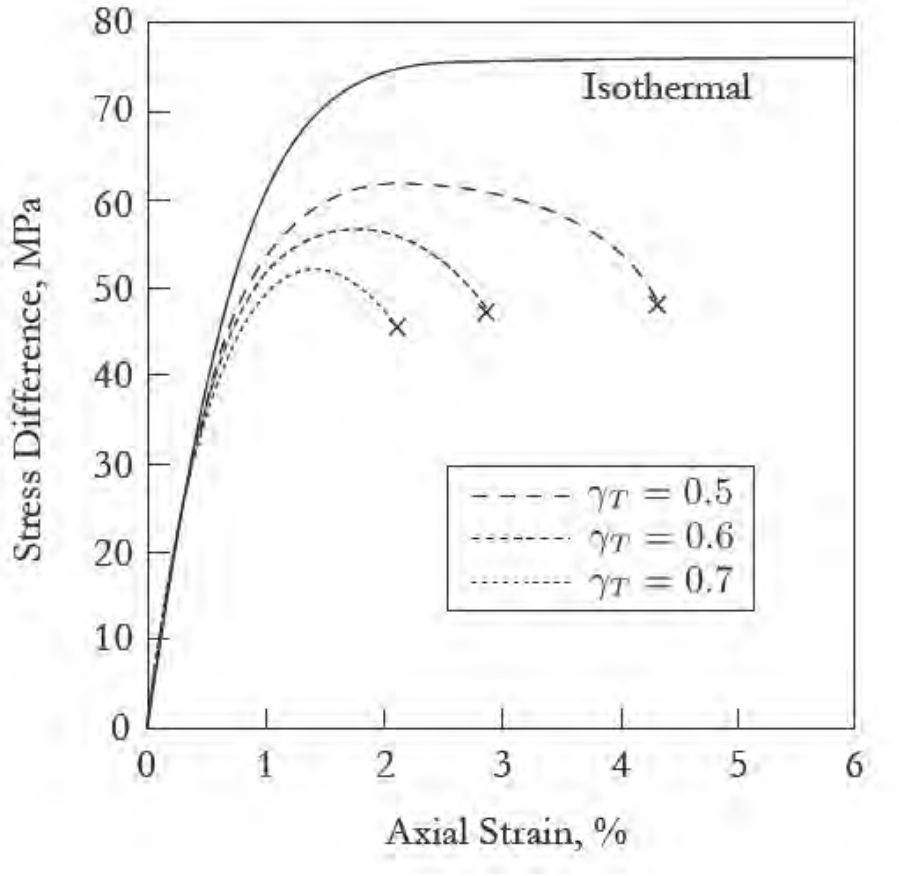

TX compression of NC Tournemire shale

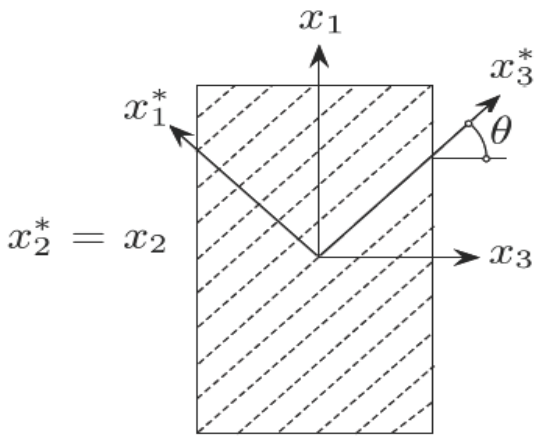

- Isothermal, at 40 MPa confining pressure, Zhao et al. (2018)
- Lab data are from Niandou et al. (1997)

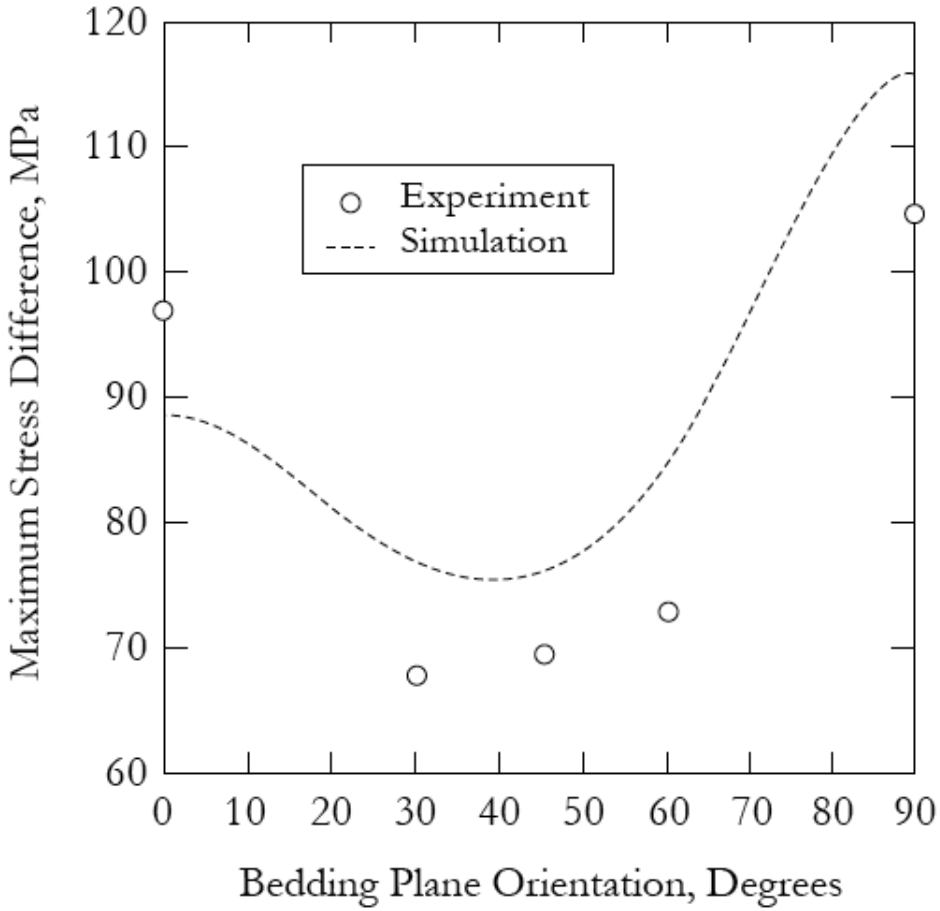

TX compression of synthetic transversely isotropic rock

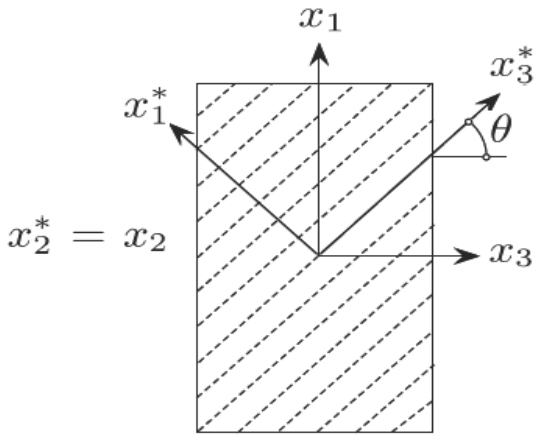

- Isothermal, at 40 MPa confining pressure, Zhao et al. (2018)
- Lab data from Tien et al. (2006)

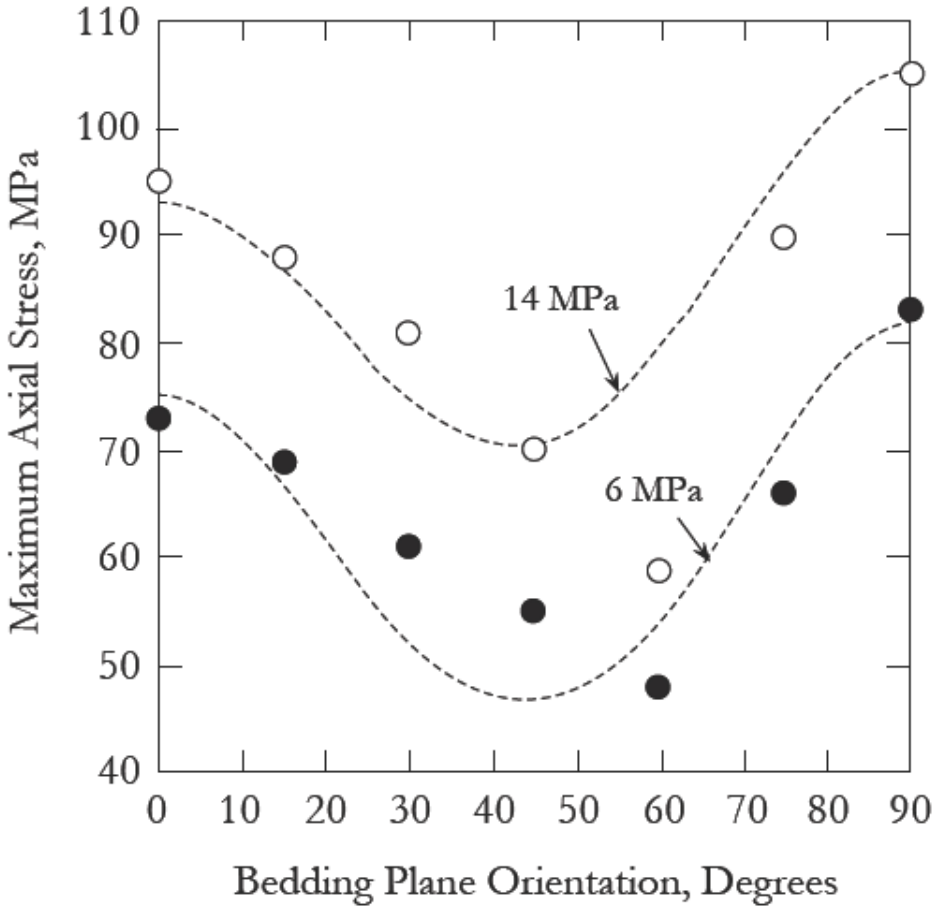

Plane strain compression of OC Tournemire shale

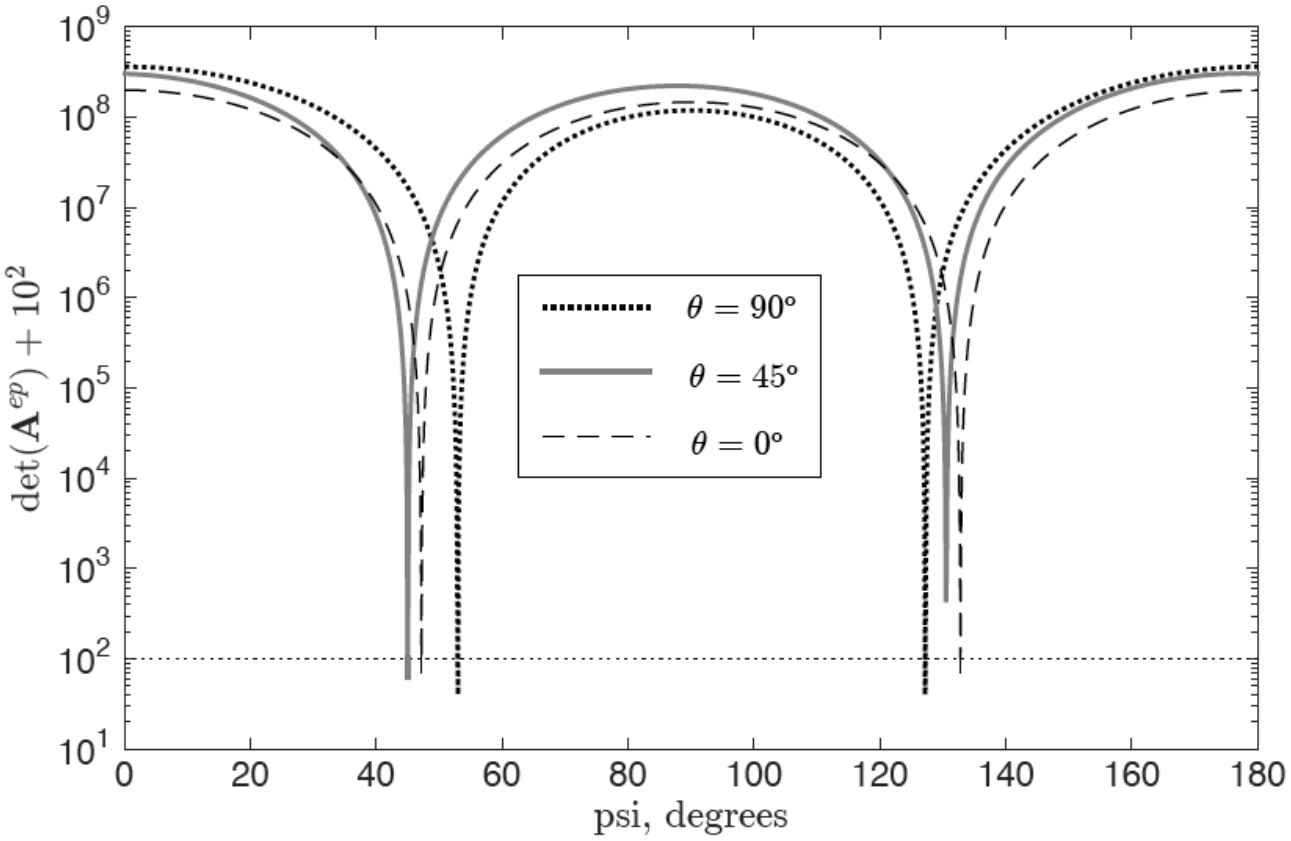

Semnani et al. (2016)

Plane strain compression of OC Tournemire shale

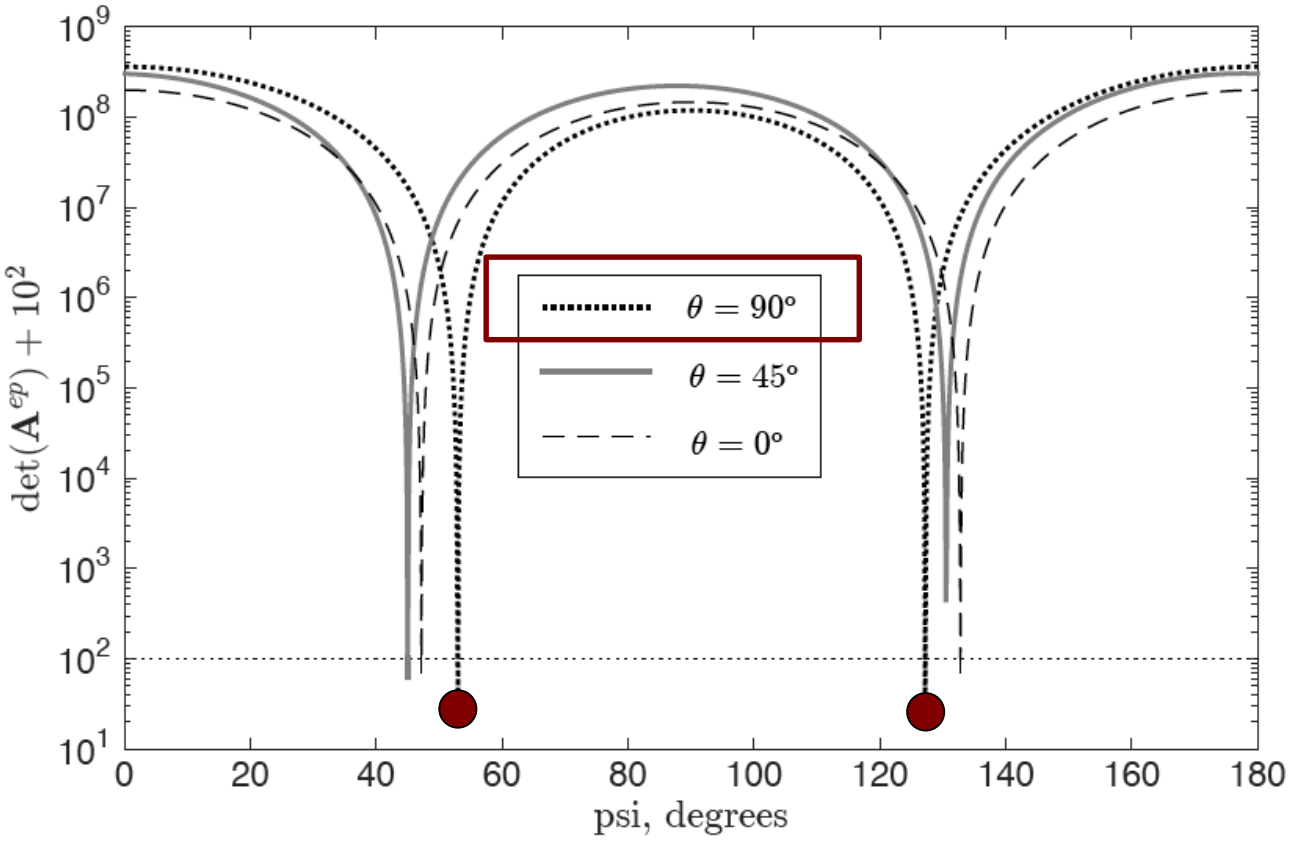

Semnani et al. (2016)

Plane strain compression of OC Tournemire shale

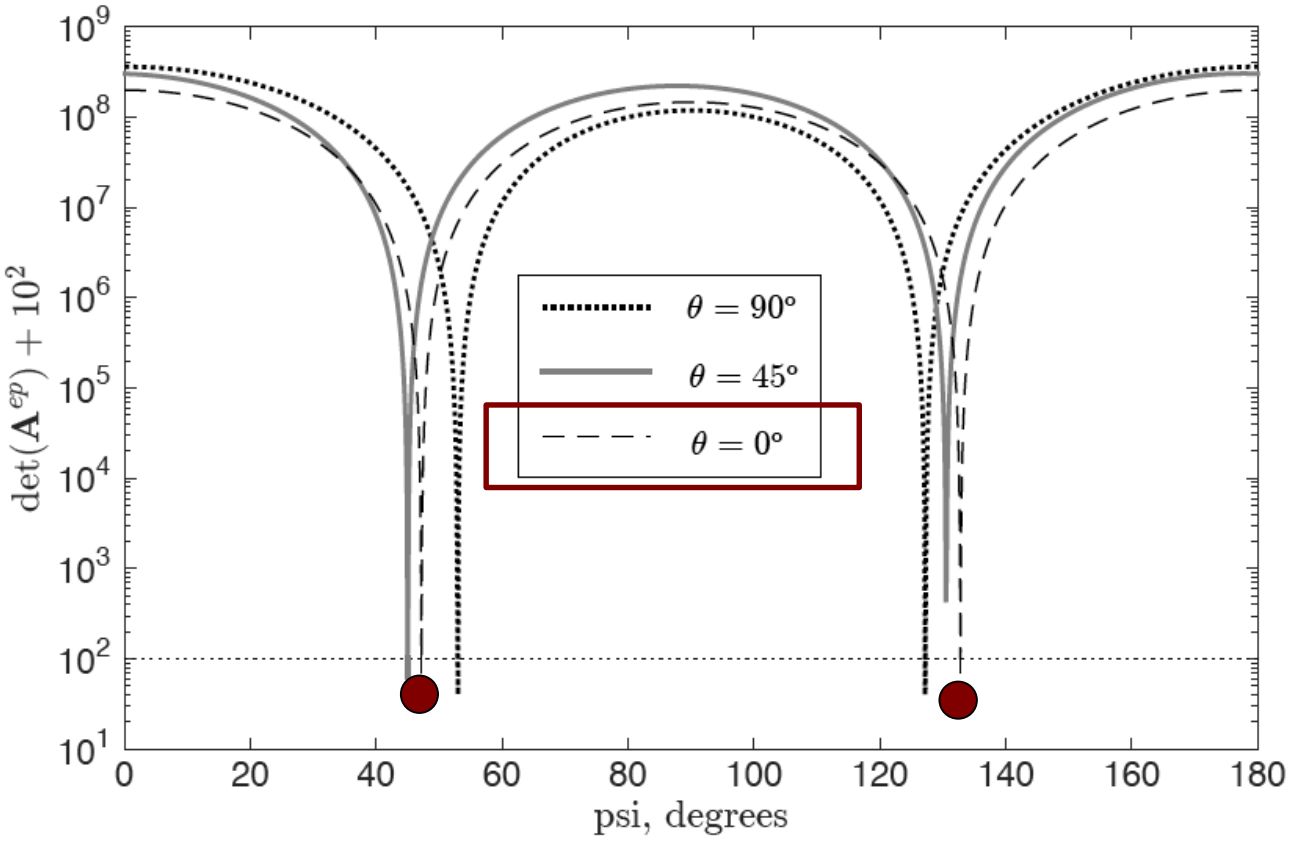

Semnani et al. (2016)

Plane strain compression of OC Tournemire shale

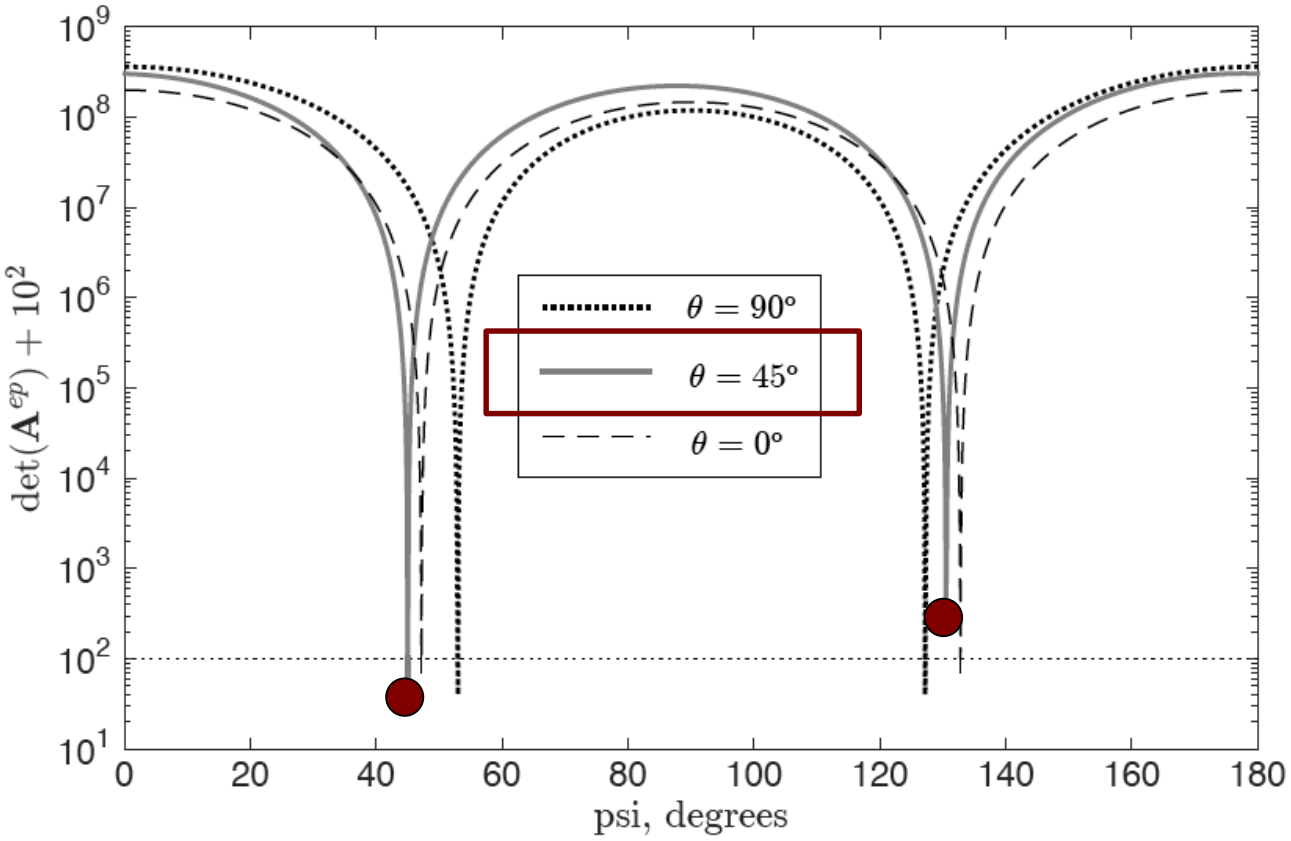

Semnani et al. (2016)

Plane strain compression of OC Tournemire shale

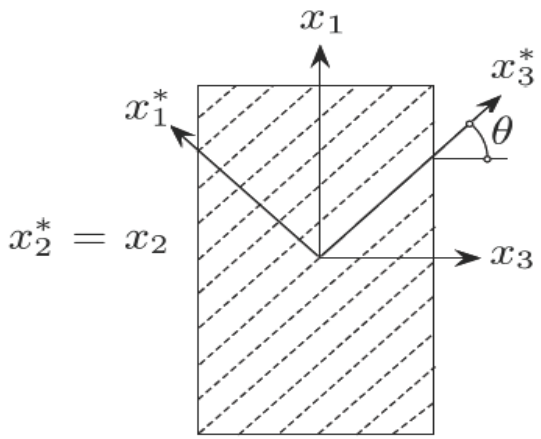

- Simulations are for OCR = 50 at 1 MPa confining stress, Zhao et al. (2018)

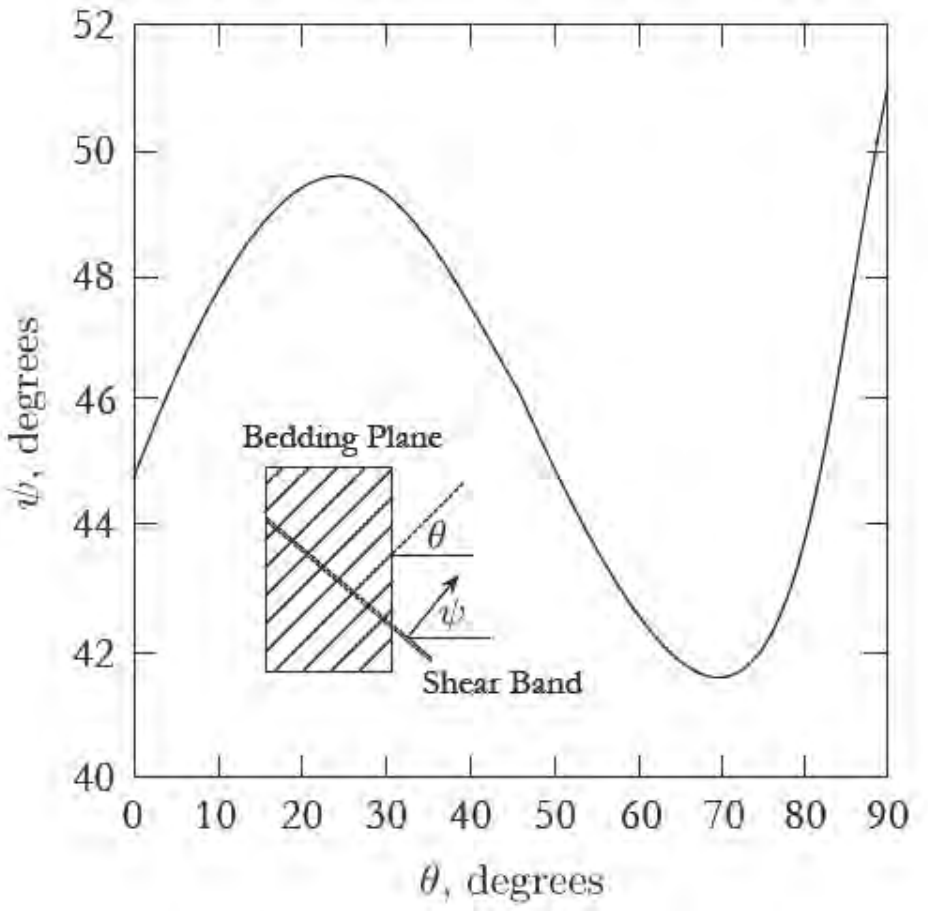

Plane strain compression of OC Tournemire shale

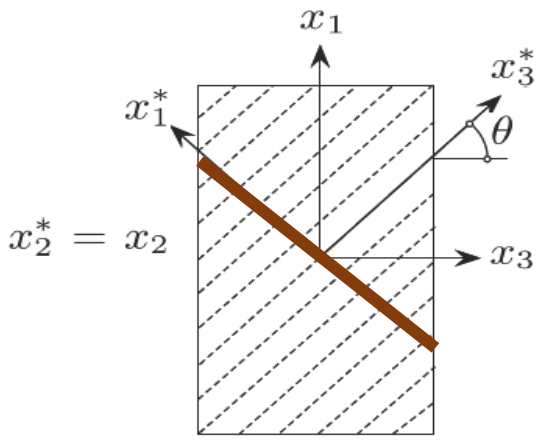

- Simulations are for OCR = 50 at 1 MPa confining stress, Zhao et al. (2018)

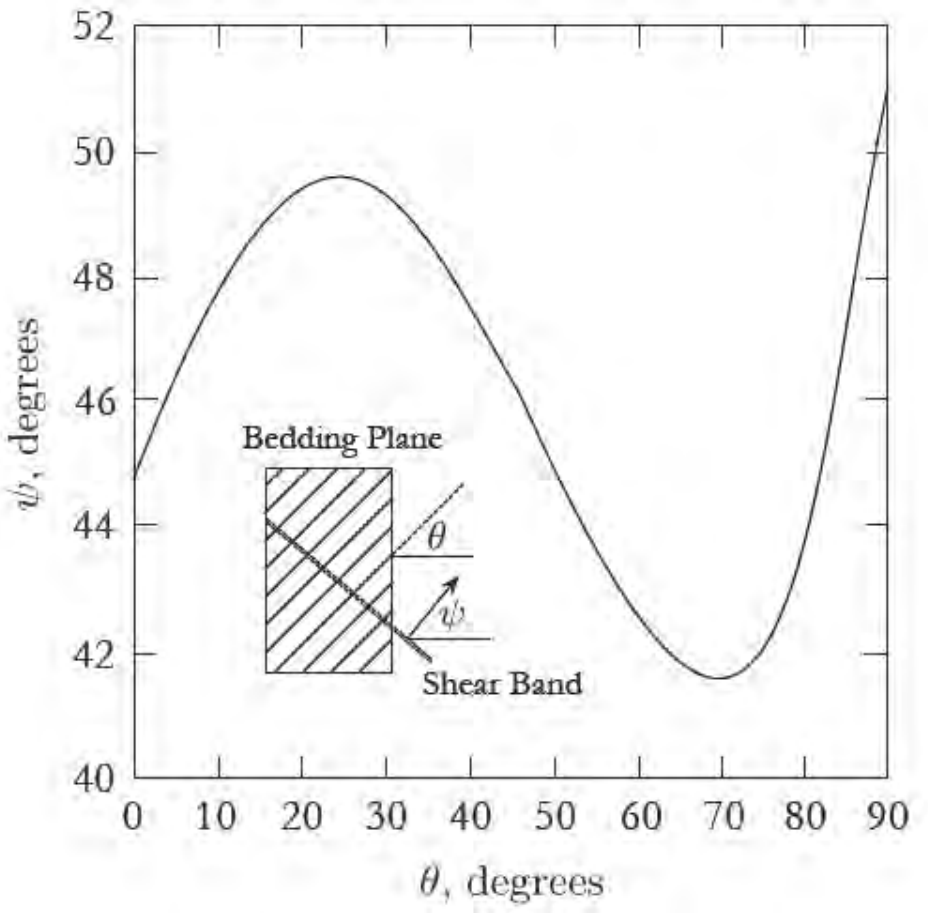

Smooth versus clamped ends

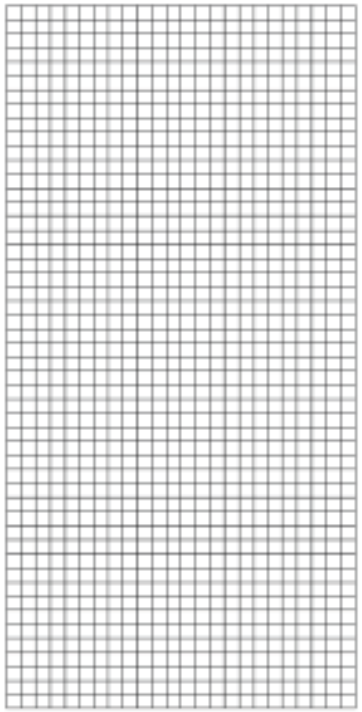

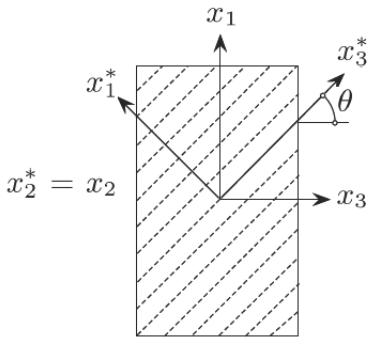

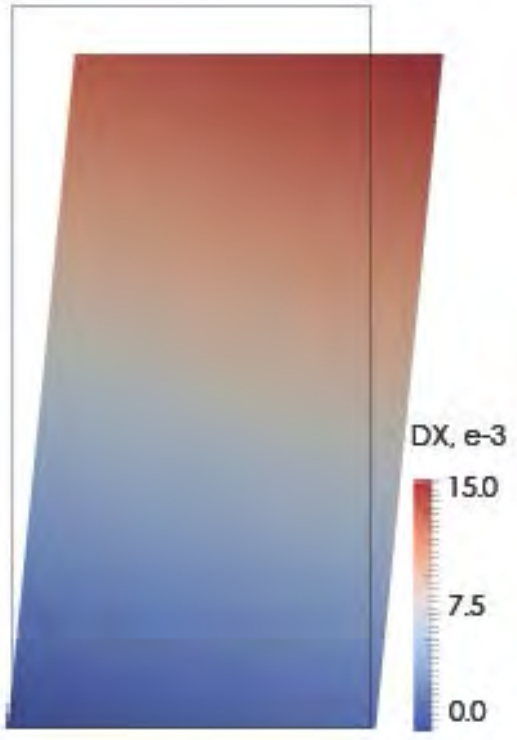

smooth ends

Zhao et al. (2018)

Smooth versus clamped ends

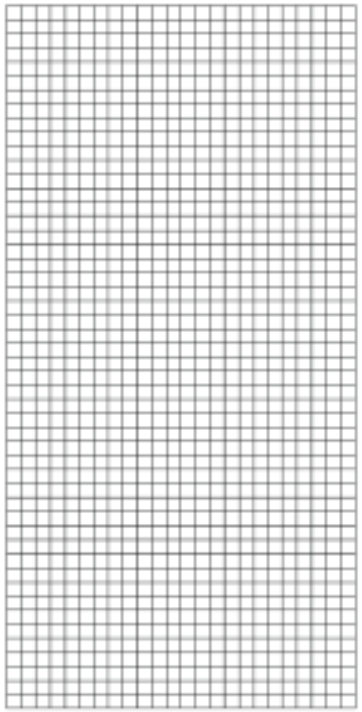

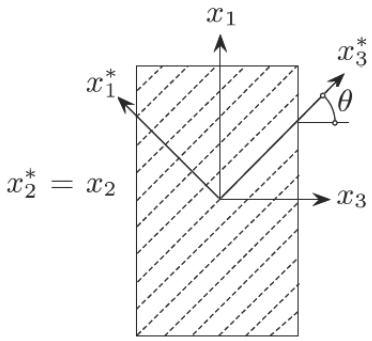

restoring force

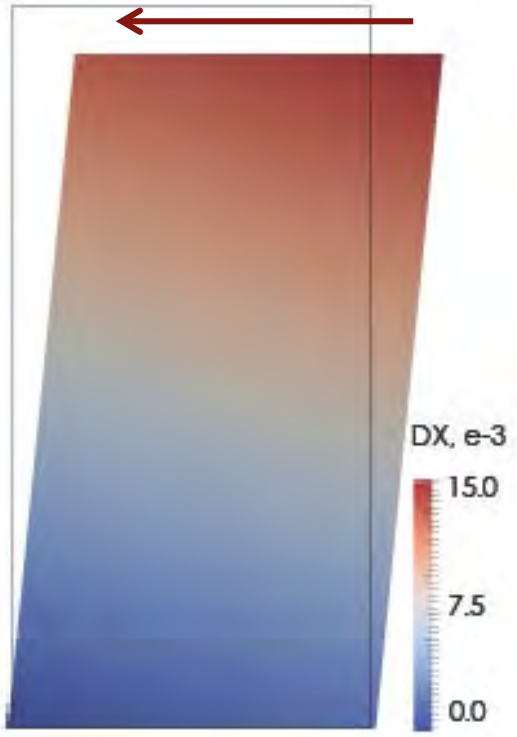

smooth ends

Zhao et al. (2018)

Smooth versus clamped ends

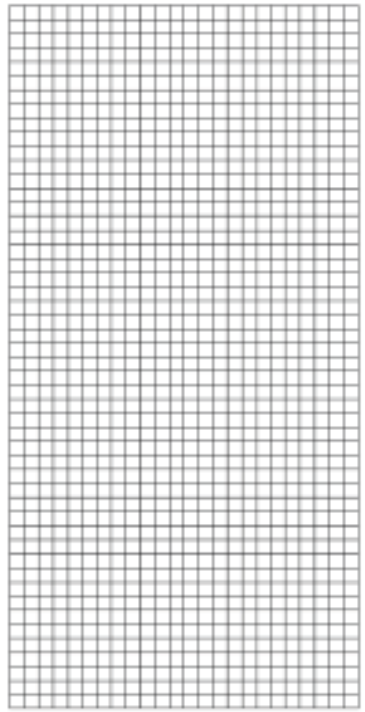

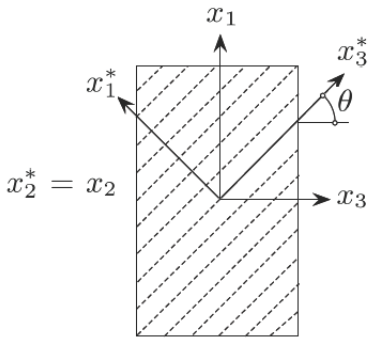

restoring force

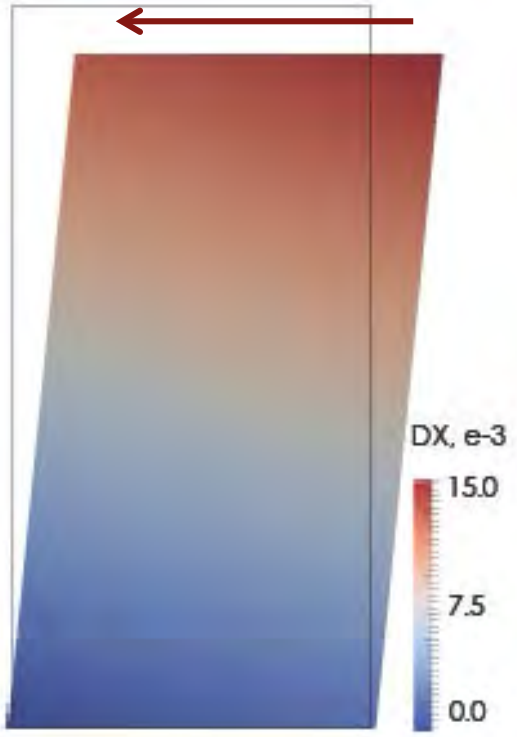

smooth ends

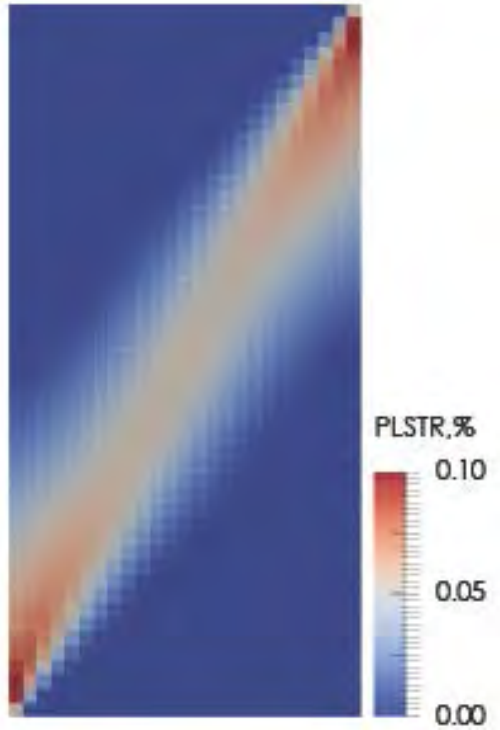

clamped ends

Zhao et al. (2018)

Smooth versus clamped ends

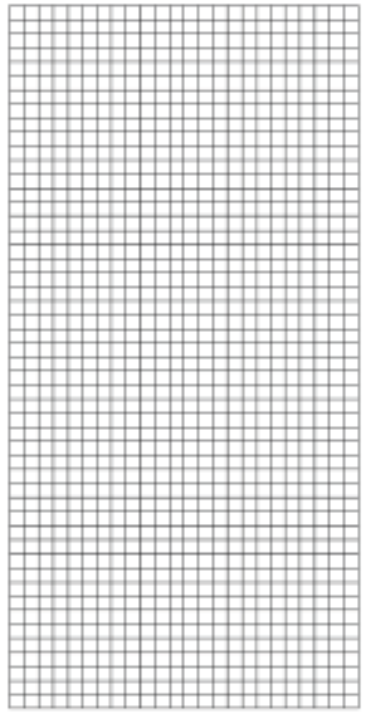

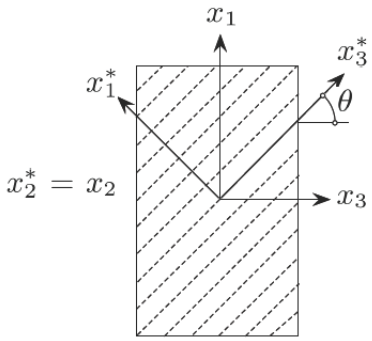

shear band direction predicted by local bifurcation

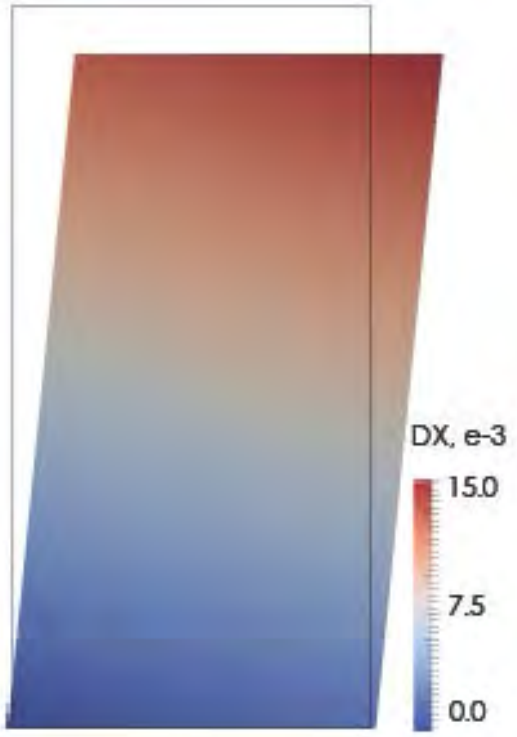

smooth ends

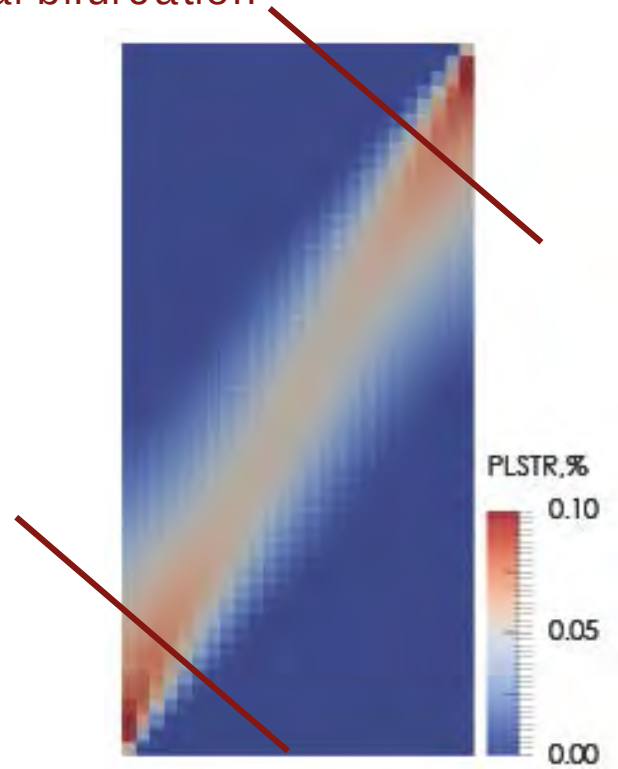

clamped ends

Zhao et al. (2018)

Smooth versus clamped ends

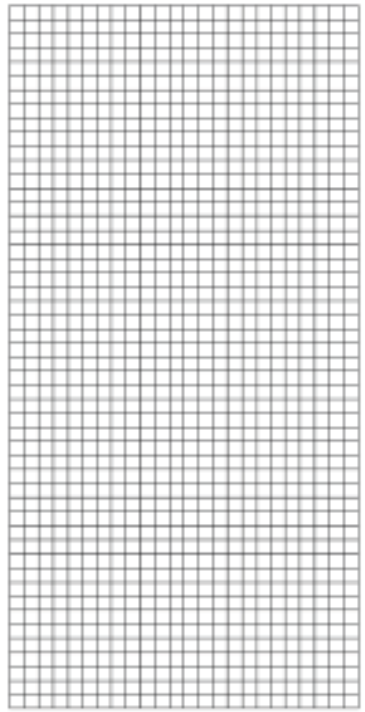

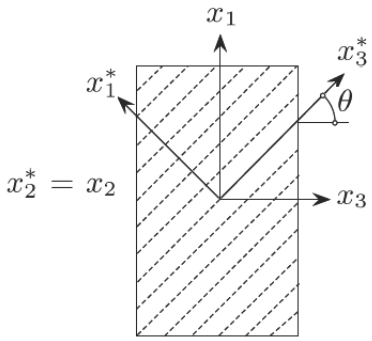

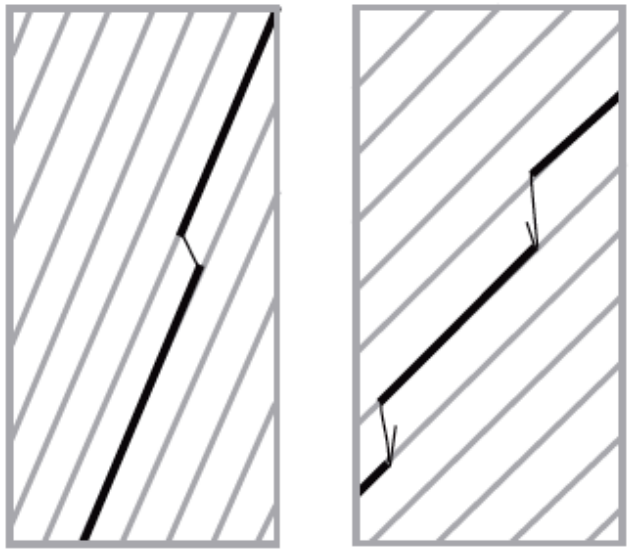

Failure modes observed in synthetic transversely isotropic rock, Tien et al. (2006)

Zhao et al. (2018)

In progress . . .

- Transverse isotropy in fluid flow and non-Darcy flow, Zhang & Borja (2019). CMAME, in press.
- Creep in shale at submicron scale – bridging nanoscale to millimeter scale, Yin & Borja (2019). CMAME.

Acknowledgments

- Collaborators: Shabnam Semnani, Joshua White, Qing Yin, Yang Zhao.

- Funding provided by the U.S. Department of Energy under Award Number DE-FG02-03ER15454 and by the U.S. National Science Foundation under Award Number CMMI-1462231.

On the strength of transversely isotropic rocks

¡Gracias!

March 29, 2019